# Strange and non-strange quark distributions

S.Alekhin (*Univ. of Hamburg & IHEP Protvino)*

- strange quarks: collider and fixed-target data
- u- and d-quarks: collider and deuteron data
- heavy quarks: FFN, VFN, and intrinsic charm

*Univ. of Washington, Seattle, 2 Oct 2017*

# Theory reminder: factorization

small distances

QPM: electro-production inclusive
structure function

$F_2(x,Q^2)=\Sigma_q\, e^2_q\, p_q(x)$

$p_q(x)$ – parton probability distributions
(PDFs)

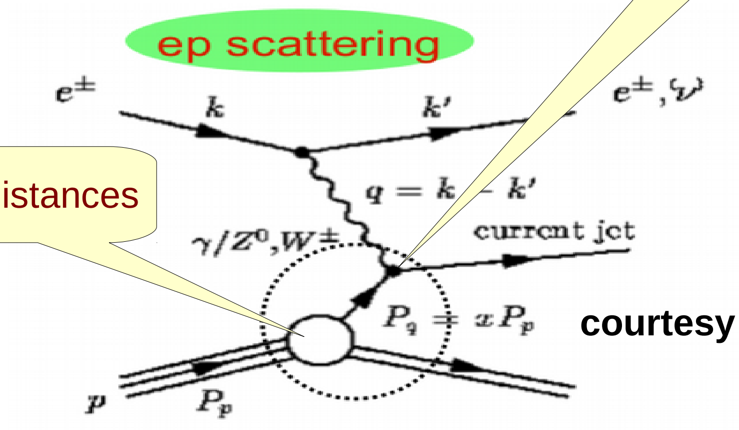


large distances

courtesy of S.Magill

QCD radiative corrections:

soft

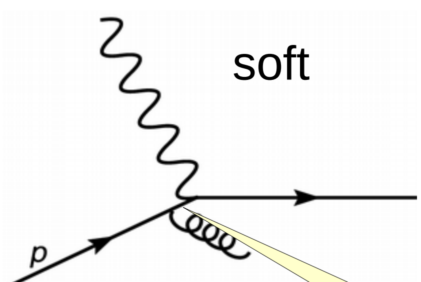


collinear

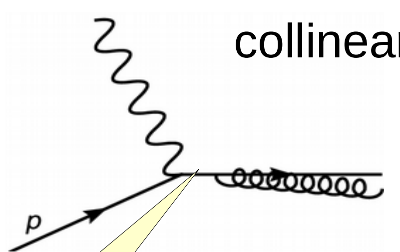


virtual

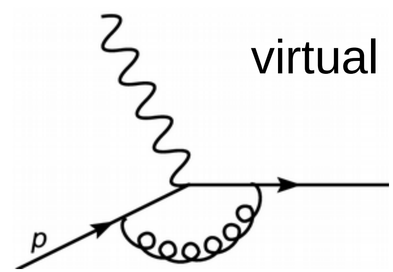


courtesy of M.H.Seymour

Mass singularity

Mass singularity appears for the massless partons,
however, t can be absorbed into PDFs ⇒ PDF evolution

Better theoretical accuracy / Scheme dependence of PDFs

State-of-art:

NNLO **Moch, Vermaseren Vogt NPB 688, 101 (2004); NPB 691, 129 (2004)**

N3LO **Moch et al. hep-ph/1707.08315; Velizhanin hep-ph/1411.1331; Baikov, Chetyrkin NPPS 160, 76 (2006)**

# Global PDF fits

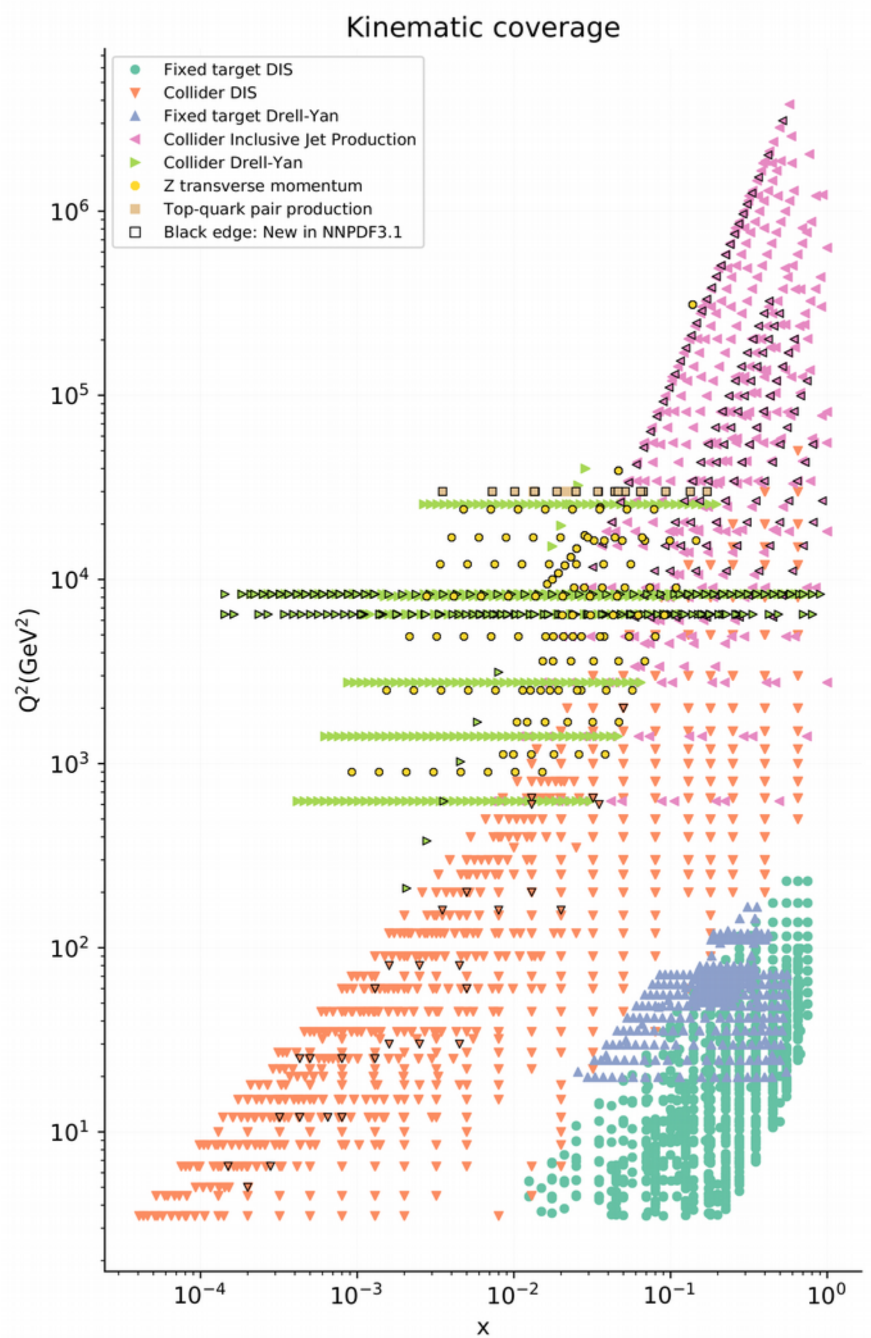


NNPDF hep-ph/1706.00428

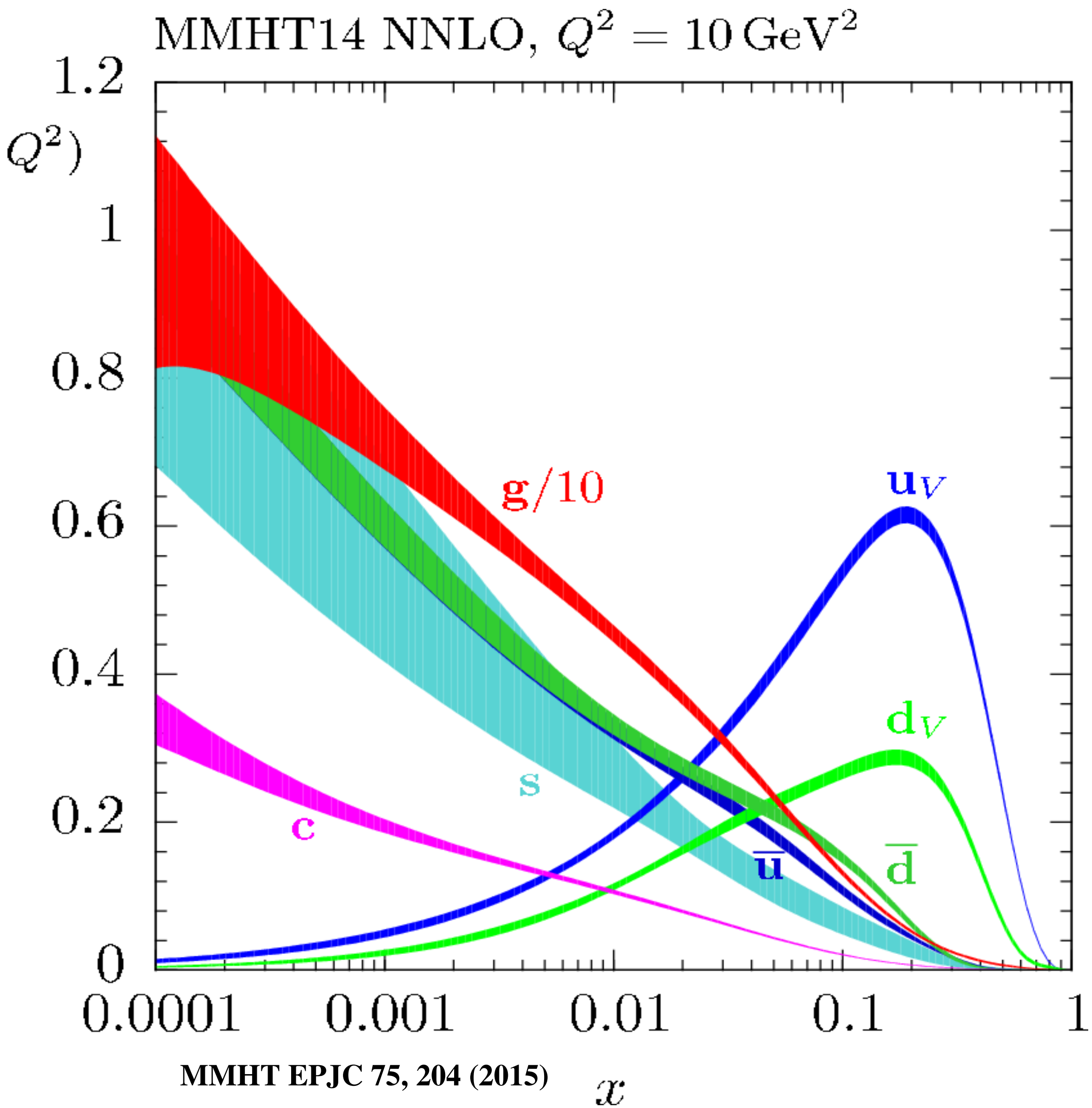


MMHT EPJC 75, 204 (2015)

Various processes provide constraints on various PDFs' combinations

# The ABMP16 fit ingredients

QCD:

- NNLO evolution
- NNLO massless DIS and DY coefficient functions
- NLO+ massive DIS coefficient functions (**FFN scheme**)
  - – NLO + NNLO(approx.) corrections for NC
  - – NNLO CC at Q>> $m_c$
  - – running mass
- NNLO exclusive DY (FEWZ 3.1)
- NNLO inclusive ttbar production ( pole / running mass )
- Relaxed form of (dbar-ubar) at small x

DATA:

- DIS NC/CC inclusive (HERA I+II added)
- DIS NC charm production (HERA)
- DIS CC charm production (HERA, NOMAD, CHORUS, NuTeV/CCFR)
- fixed-target DY
- LHC DY distributions (ATLAS, CMS, LHCb)
- t-quark data from the LHC and Tevatron
- deuteron data are excluded

Power corrections:

- target mass effects
- dynamical twist-4 terms

**sa, Blümlein, Moch, Plačakytė PRD 96, 014011 (2017)**
**…...**

# Strange sea from the νN DIS

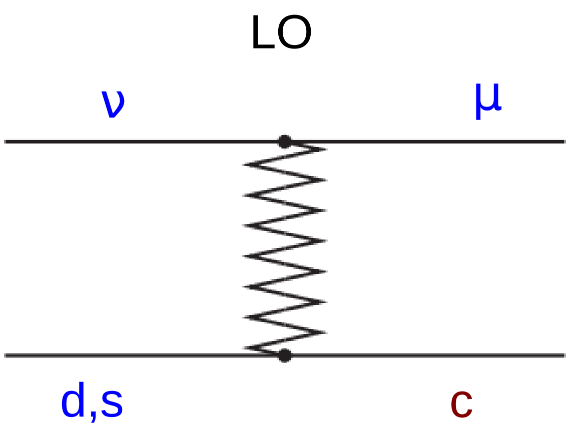


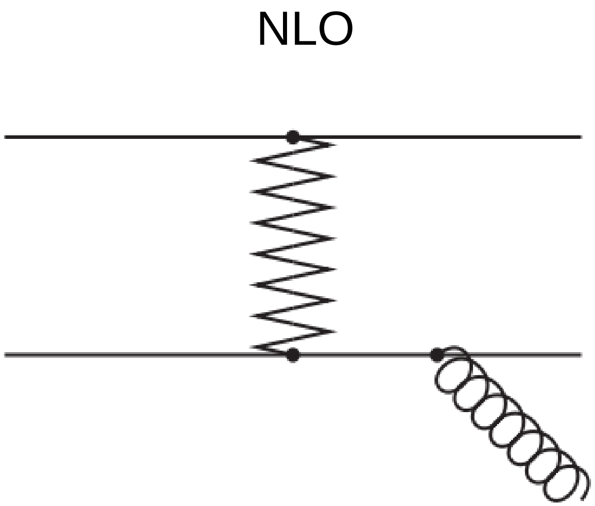


Two decay modes of c-quark are used: hadronic (emulsion experiments) and semi-leptonic (electronic experiments)

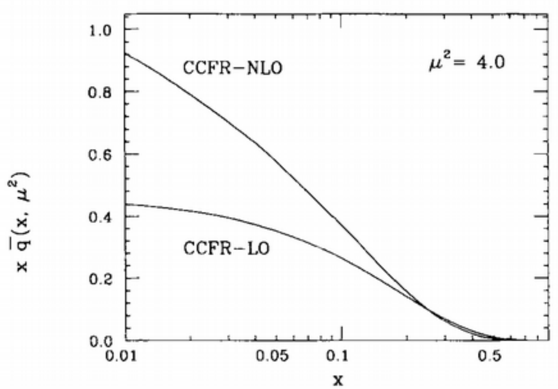


**Fig. 3.** The quark sea distribution $x\bar{q}(x, \mu^2 = 4.0\,\mathrm{GeV}^2/c^2)$ determined at next-to-leading order and leading order

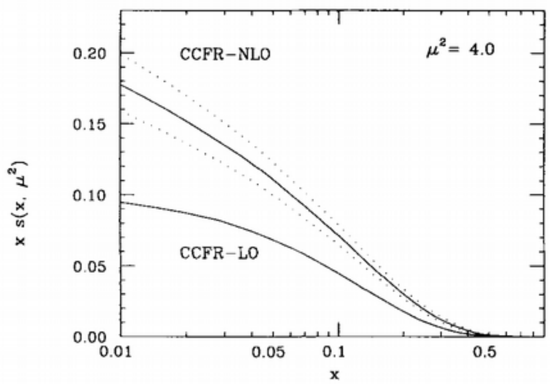


**Fig. 4.** The strange quark distribution $xs(x, \mu^2 = 4.0\,\mathrm{GeV}^2/c^2)$ determined at next-to-leading order (described in section 4.1) and leading order. The band around the NLO curve indicates the $\pm 1\sigma$ uncertainty in the distribution

**CCFR ZPC 65, 189 (1995)**

Primary source for the strange sea was for a long time neutrino-induced charm production measured by CCFR/NuTeV at Fermilab preferring a suppression of ~0.5 w.r.t. non-strange sea

# NuTeV/CCFR data in the PDF fit framework

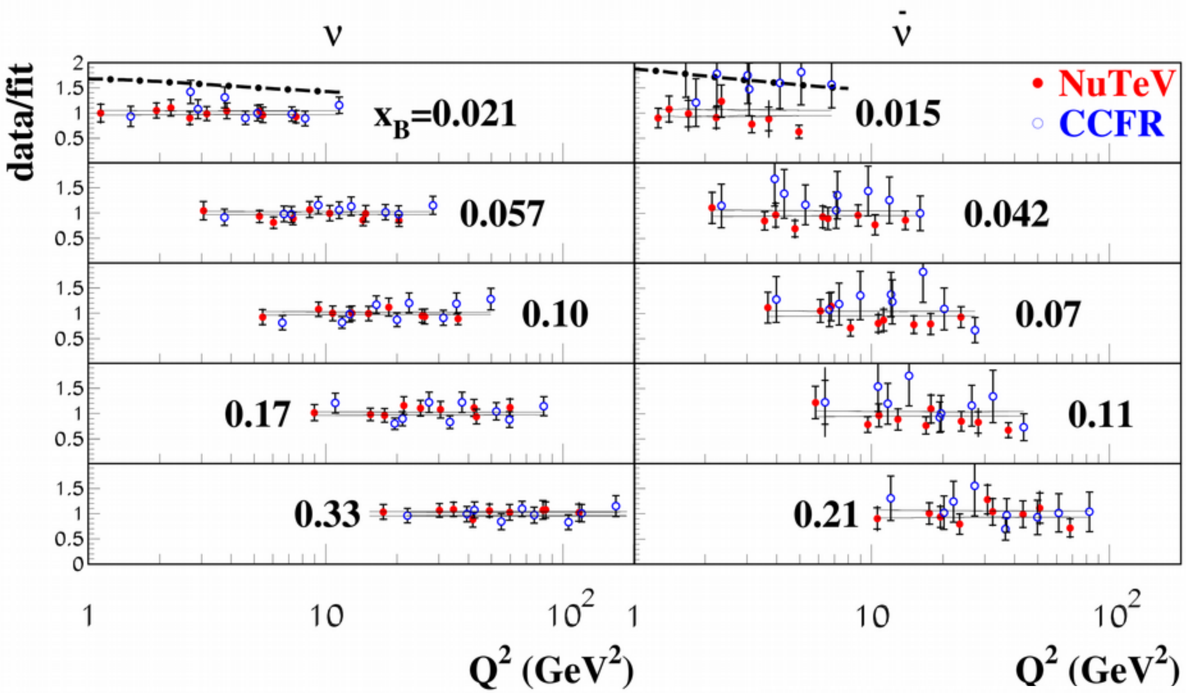


- CCFR and NuTeV are in a good agreement
- Charge asymmetry in the strange sea is consistent with 0 within uncertainties

sa, Kulagin, Petti PLB 675, 433 (2009)

$$\kappa_s(\mu^2) = \frac{\int_0^1 x[s(x,\mu^2)+\bar{s}(x,\mu^2)]dx}{\int_0^1 x[\bar{u}(x,\mu^2)+\bar{d}(x,\mu^2)]dx},$$

*Integral suppression factor*
*$K_s$(20 GeV$^2$)=0.62±0.04 is obtained*

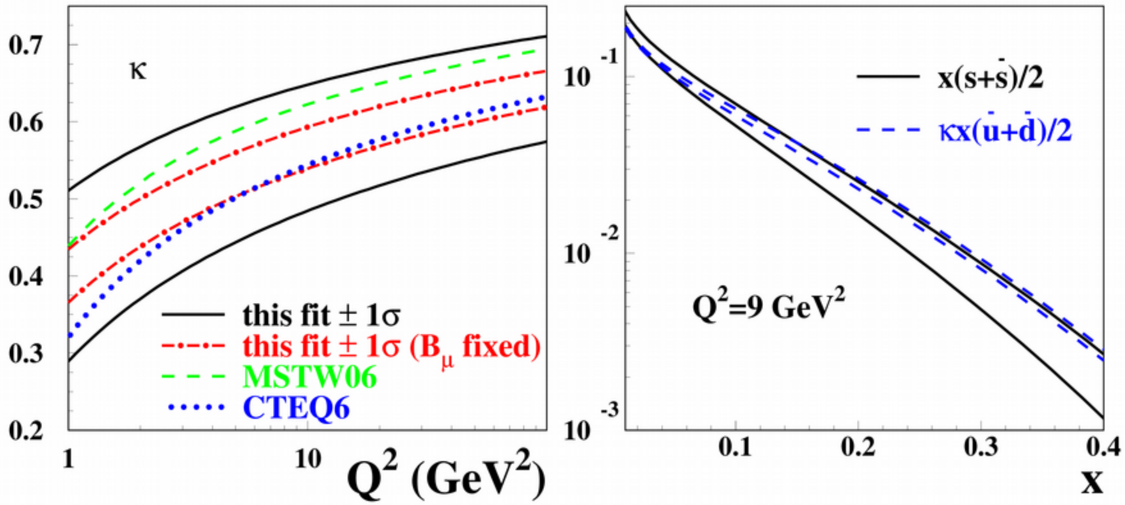

# NOMAD charm data

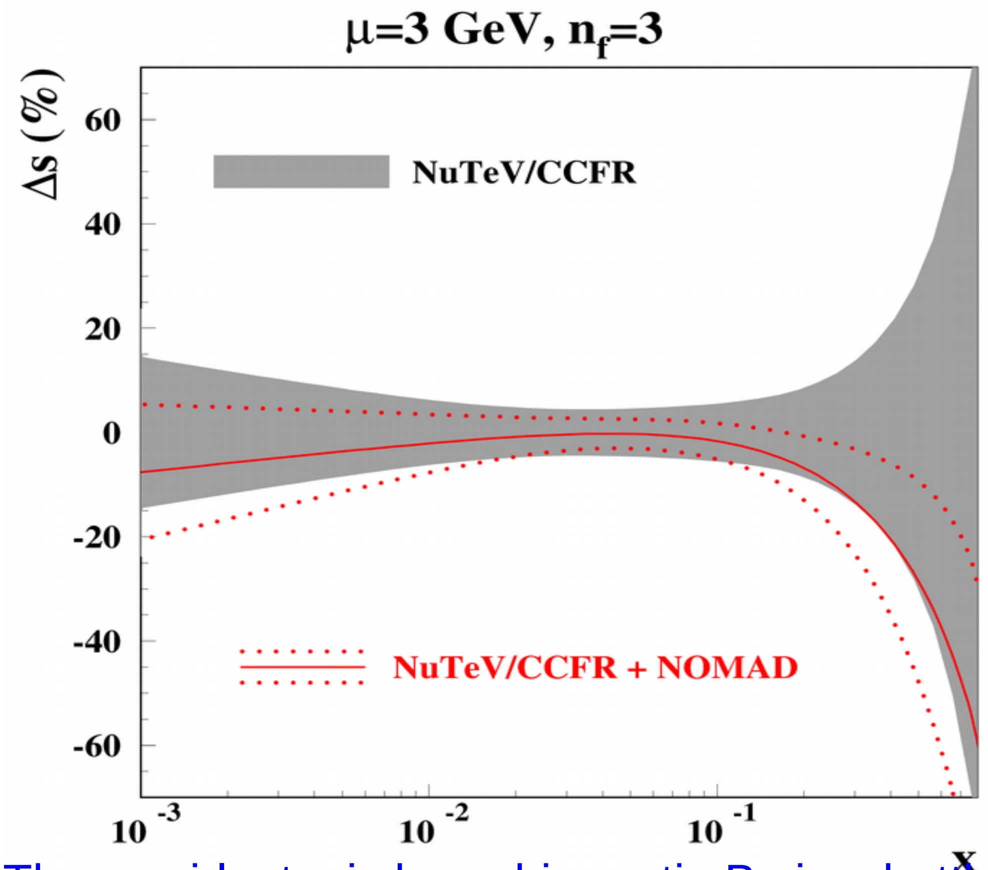


NOMAD NPB 876, 339 (2013)

- The data on ratio 2μ/incl. CC ratio with the 2μ statistics of 15000 events (much bigger than in earlier CCFR and NuTeV samples).
- Systematics, nuclear corrections, etc. cancel in the ratio
- Pull down strange quarks at x>0.1 with a sizable uncertainty reduction

The semi-leptonic branching ratio $B_\mu$ is a bottleneck

– weighted average of the charmed-hadron rates

$$B_\mu(E_\nu)=\sum_h r^h(E_\nu)B^h_\mu = a/(1+b/E_\nu)$$

– fitted simultaneously with the PDFs, etc. using the constraint from the emulsion data

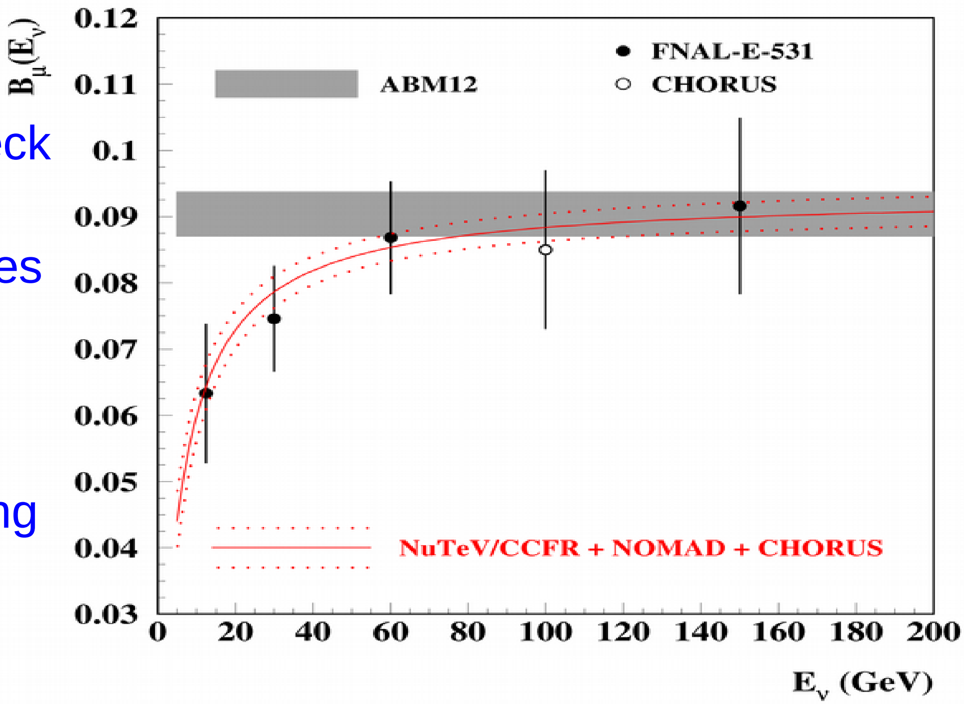

# Impact of NOMAD data

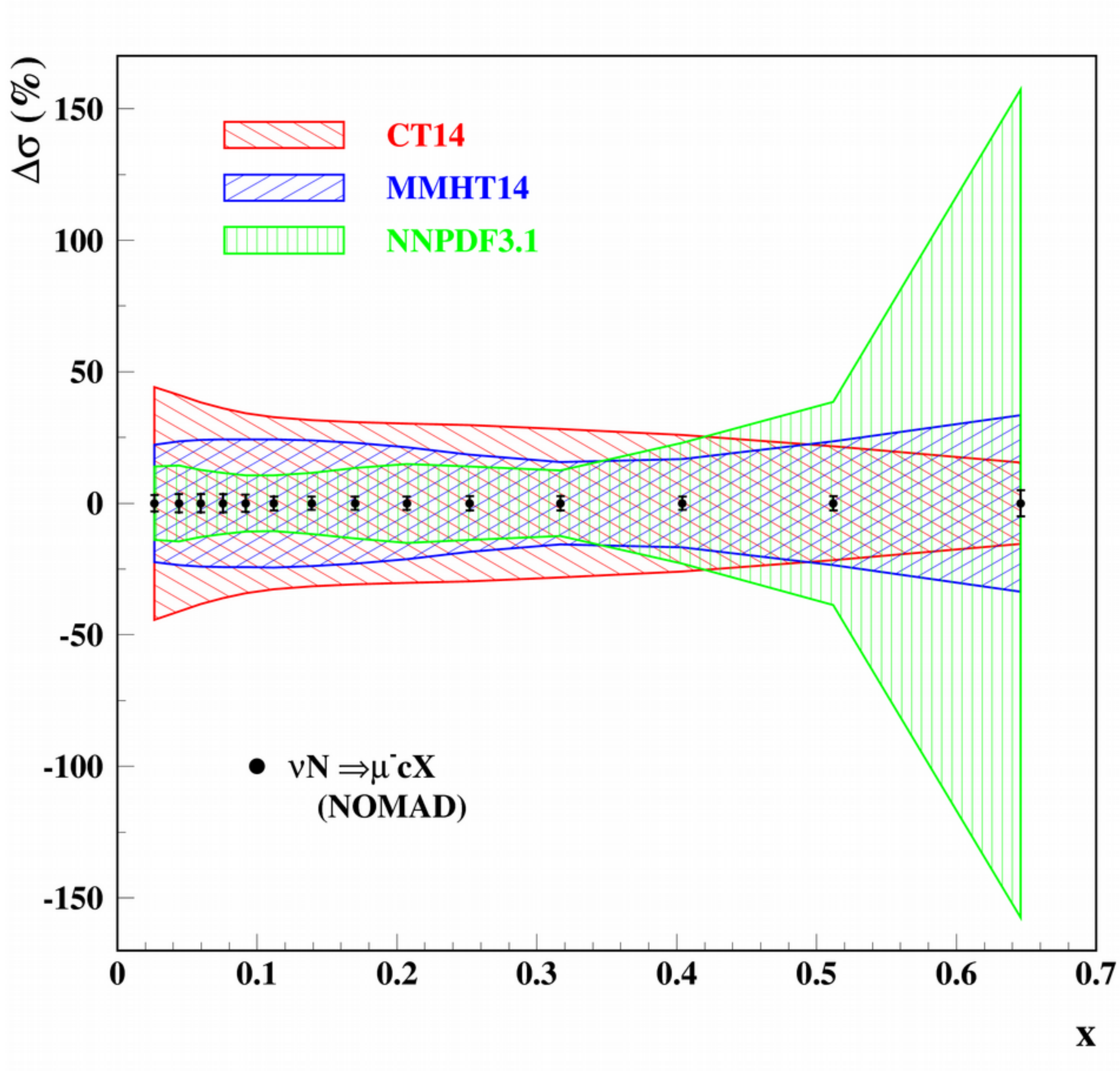


- Evident room for the PDF improvement by adding NOMAD data to various PDF fits
- Big spread in the predictions ⇒ PDF4LHC averaging provides inefficient estimate

# Comined Run I+II HERA data

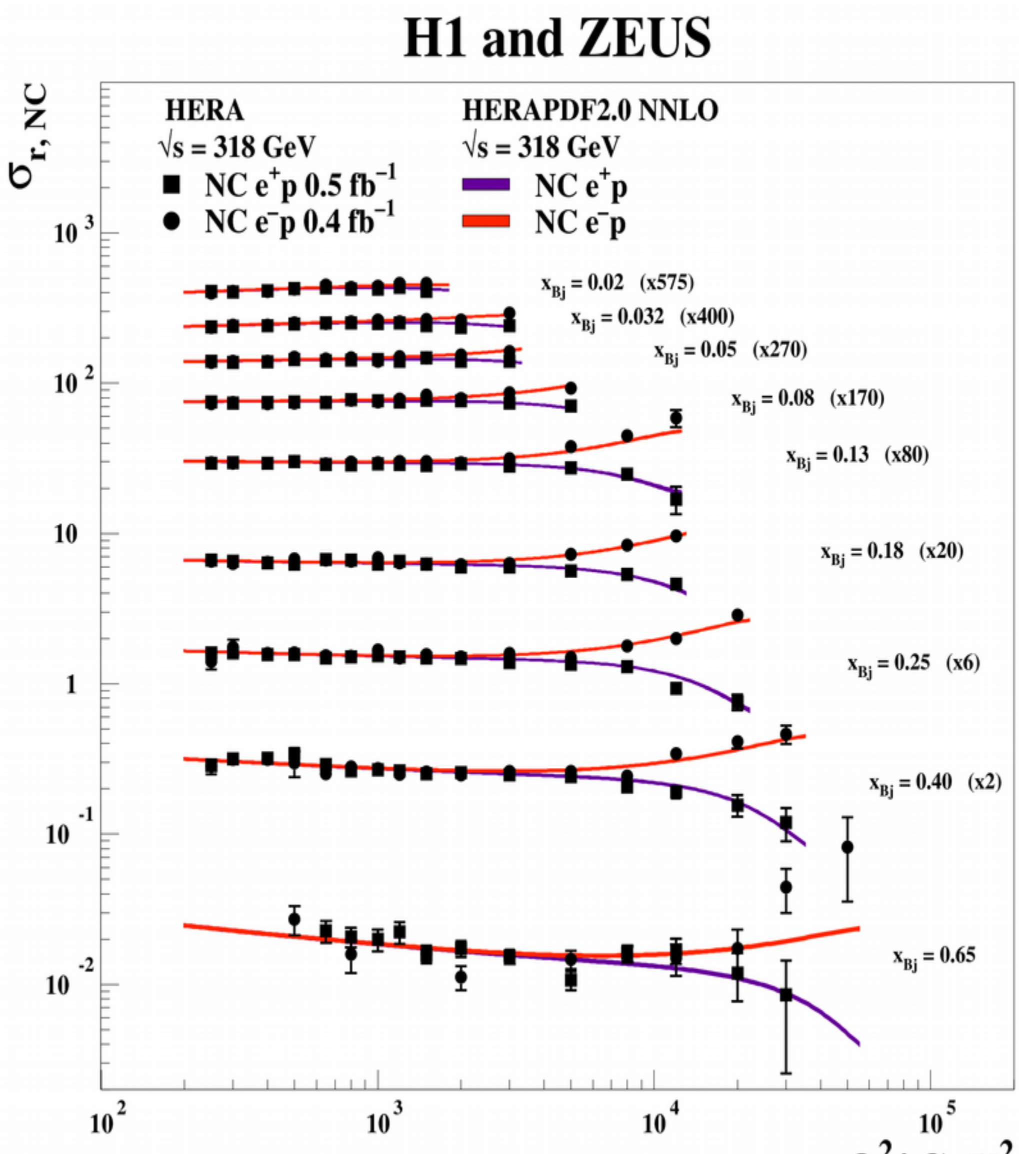


H1 and ZEUS EPJC 75, 580 (2015)

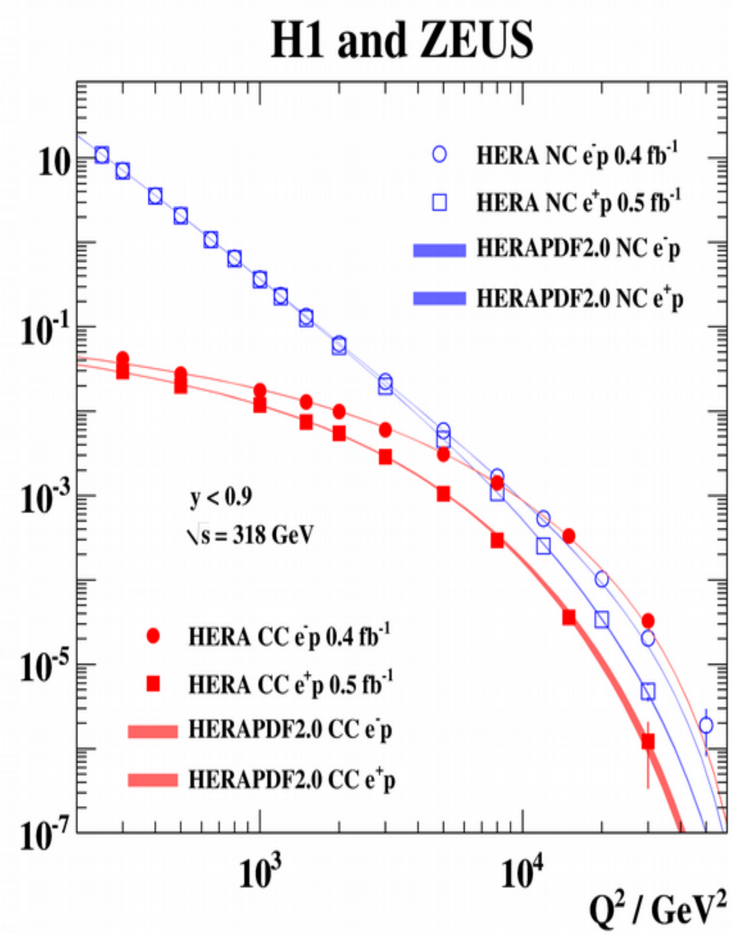


- σ(DIS) ~ $q_u^2u(x) + q_d^2d(x) + q_s^2s(x)$ ⇒ poor separation of the quark species
- The deuteron fixed-target data (SLAC, BCDMS NMS) help to disentangle d- and u-distributions due to transmutation u⇔d

# Forward DY kinematics at Tevatron and the LHC

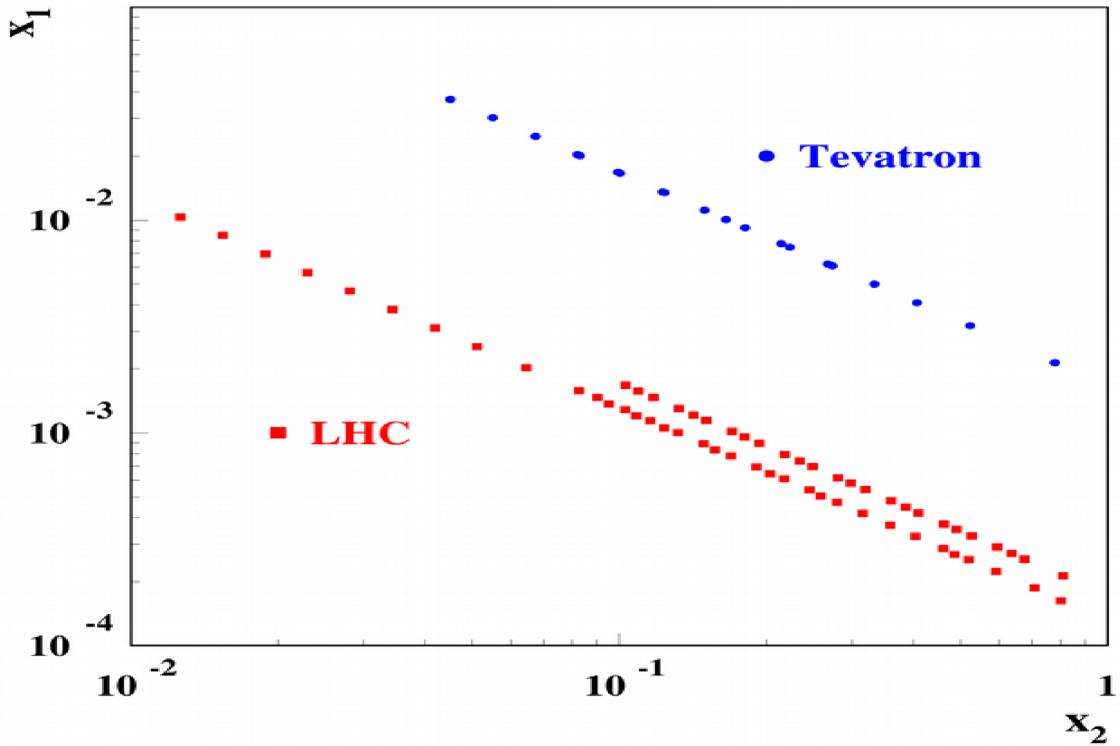


In the forward region $x_2 >> x_1$

$\sigma(W^+) \sim u(x_2)\, \mathrm{dbar}\, (x_1)$

$\sigma(W^-) \sim d(x_2)\, \mathrm{ubar}(x_1)$

$\sigma(Z) \sim Q_U^2 u(x_2)\, \mathrm{ubar}\, (x_1) + Q_D^2 d(x_2)\, \mathrm{dbar}(x_1)$

$\sigma(DIS) \sim q_u^2 u(x_2) + q_d^2 d(x_2)$

*Forward W&Z production probes small/large x and is complementary to the DIS ⇒ good quark disentangling*

- Fully differential kinematics; existing NNLO codes, DYNNLO and FEWZ requre huge computing resources to achieve the promille accuracy required

- DYNNLO-FEWZ difference not fully resolved

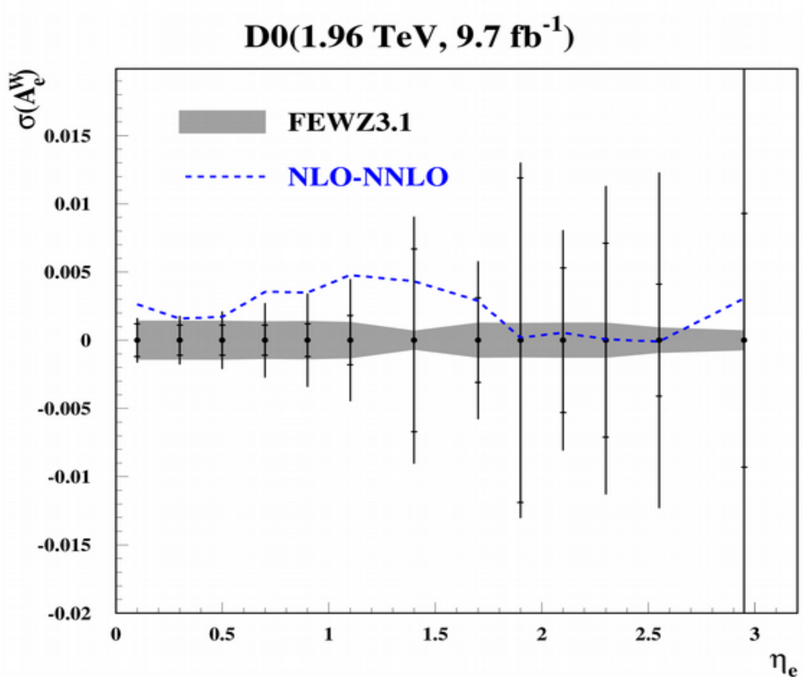


**Salam ATLAS SM workshop 2014**

**Yannick Ulrich, Barchelor thesis, Univ. of Hamburg 2015**

# Most recent DY inputs

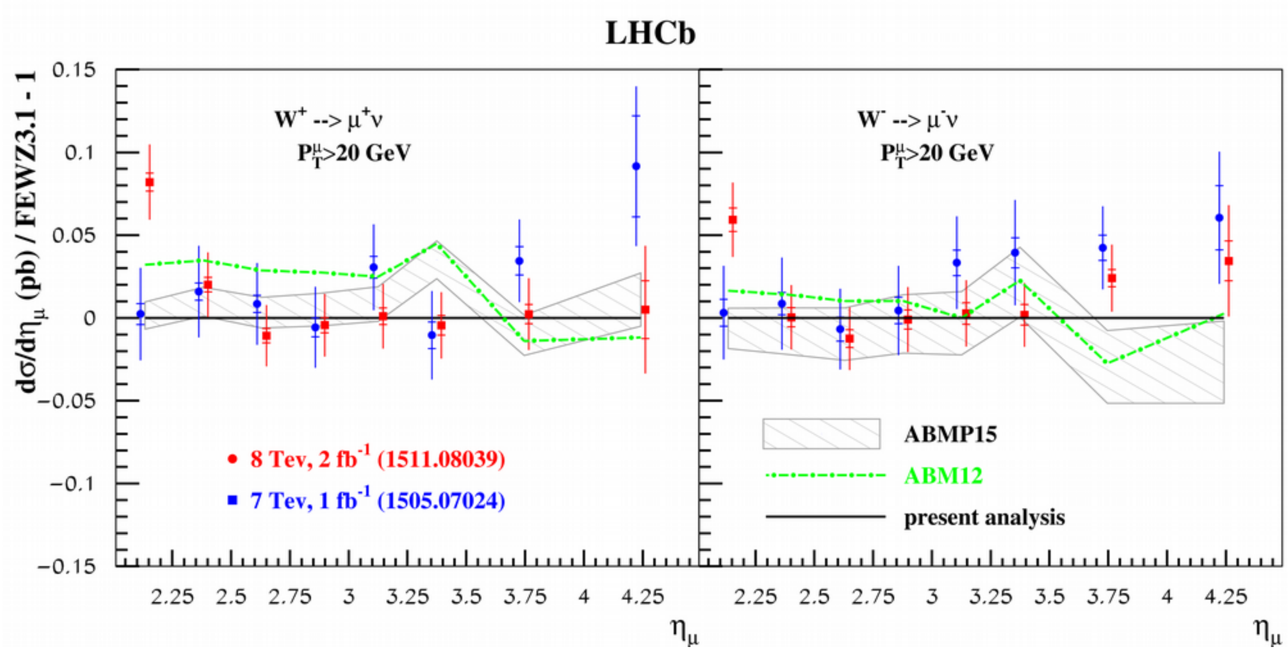


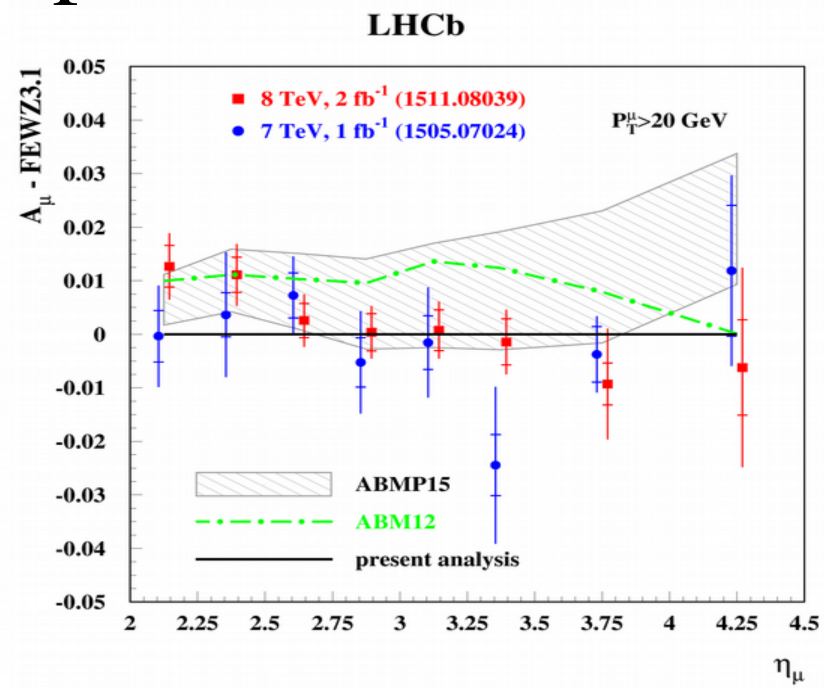


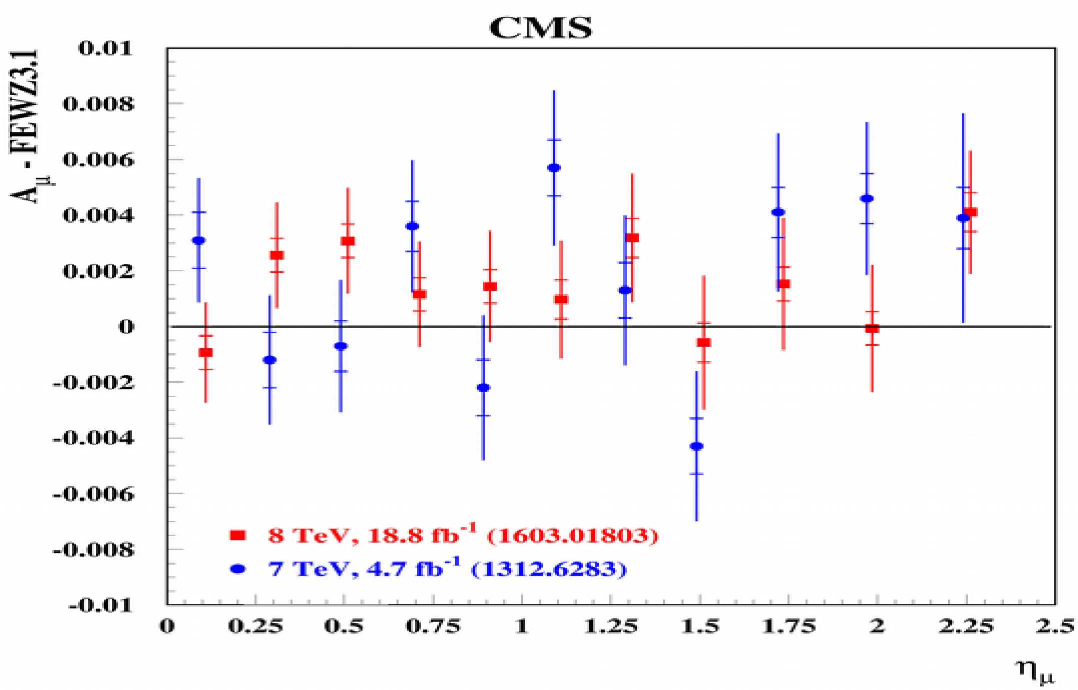


Filtering of the LHCb data has been performed:

– a bump at 7 Tev and Y=3.275 (not confirmed by the LHCb data at 8 TeV)

– and excess at 8 TeV and Y=2.125 (not confirmed by the CMS data at 8 TeV)

The CMS data at 8 TeV are much smoother than the ones at 7 TeV:

$\chi^2$=17/22 versus 22/11

# DY data selection in the ABMP16 fit

| Experiment | ATLAS | | CMS | | DØ | | LHCb | | |
|---|---|---|---|---|---|---|---|---|---|
| $\sqrt{s}$ (TeV) | 7 | 13 | 7 | 8 | 1.96 | | 7 | 8 | |
| Final states | $W^+ \to l^+\nu$<br>$W^- \to l^-\nu$<br>$Z \to l^+l^-$ | $W^+ \to l^+\nu$<br>$W^- \to l^-\nu$<br>$Z \to l^+l^-$ | $W^+ \to \mu^+\nu$<br>$W^- \to \mu^-\nu$<br>(asym) | $W^+ \to \mu^+\nu$<br>$W^- \to \mu^-\nu$ | $W^+ \to \mu^+\nu$<br>$W^- \to \mu^-\nu$<br>(asym) | $W^+ \to e^+\nu$<br>$W^- \to e^-\nu$<br>(asym) | $W^+ \to \mu^+\nu$<br>$W^- \to \mu^-\nu$<br>$Z \to \mu^+\mu^-$ | $Z \to e^+e^-$ | $W^+ \to \mu^+\nu$<br>$W^- \to \mu^-\nu$<br>$Z \to \mu^+\mu^-$ |
| Cut on the lepton $P_T$ | $P_T^l > 20$ GeV | $P_T^e > 25$ GeV | $P_T^\mu > 25$ GeV | $P_T^\mu > 25$ GeV | $P_T^\mu > 25$ GeV | $P_T^e > 25$ GeV | $P_T^\mu > 20$ GeV | $P_T^e > 20$ GeV | $P_T^\mu > 20$ GeV |
| Luminosity (1/fb) | 0.035 | 0.081 | 4.7 | 18.8 | 7.3 | 9.7 | 1 | 2 | 2.9 |
| *NDP* | 30 | 6 | 11 | 22 | 10 | 13 | 31(33) [a] | 17 | 32(34) |
| ABMP16 | 31.0 | 9.2 | 22.4 | 16.5 | 17.6 | 19.0 | 45.1(54.4) | 21.7 | 40.0(59.2) |
| CJ15 | – | – | – | – | 20 | 29 | – | – | – |
| CT14 | 42 | – | – [b] | – | – | 34.7 | – | – | – |
| HERAFitter | – | – | – | – | 13 | 19 | – | – | – |
| MMHT16 | 39 [c] | – | – | 21 | 21 [c] | 26 | (43) | 29 | (59) |
| NNPDF3.1 | 29 | – | 19 | – | 16 | 35 | (59) | 19 | (47) |

[a] The values of NDP and $\chi^2$ correspond to the unfiltered samples.
[b] For the statistically less significant data with the cut of $P_T^\mu > 35$ GeV the value of $\chi^2 = 12.1$ was obtained.
[c] The value obtained in MMHT14 fit.

- Many early low-statistical Tevatron and LHC data are not included into the fit

- The D0 sample for the charge-lepton asymmetry is preferred as compared to the W-asymmetry: smaller sensitivity to the modeling details; might even introduce a bias due to data sets' discrepancy

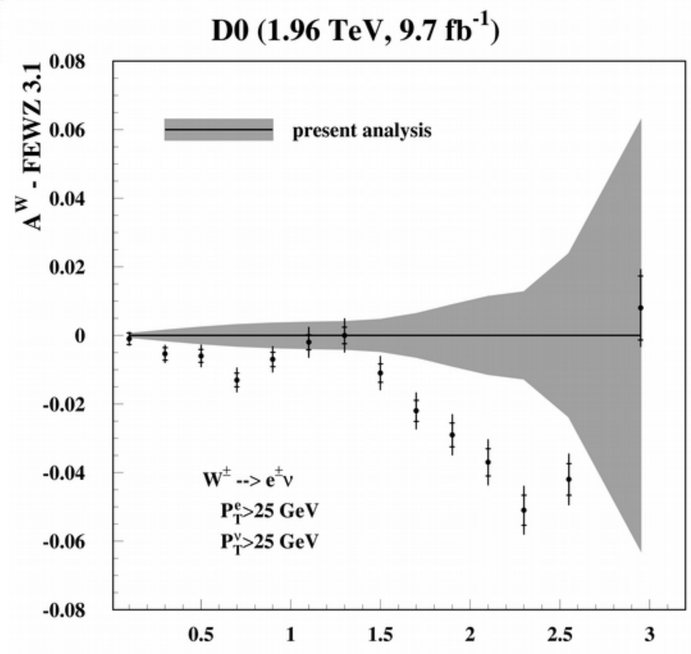


sa, Blümlein, Moch, Plačakytė PRD 94, 114038 (2016)

# Comparison of various PDF fits

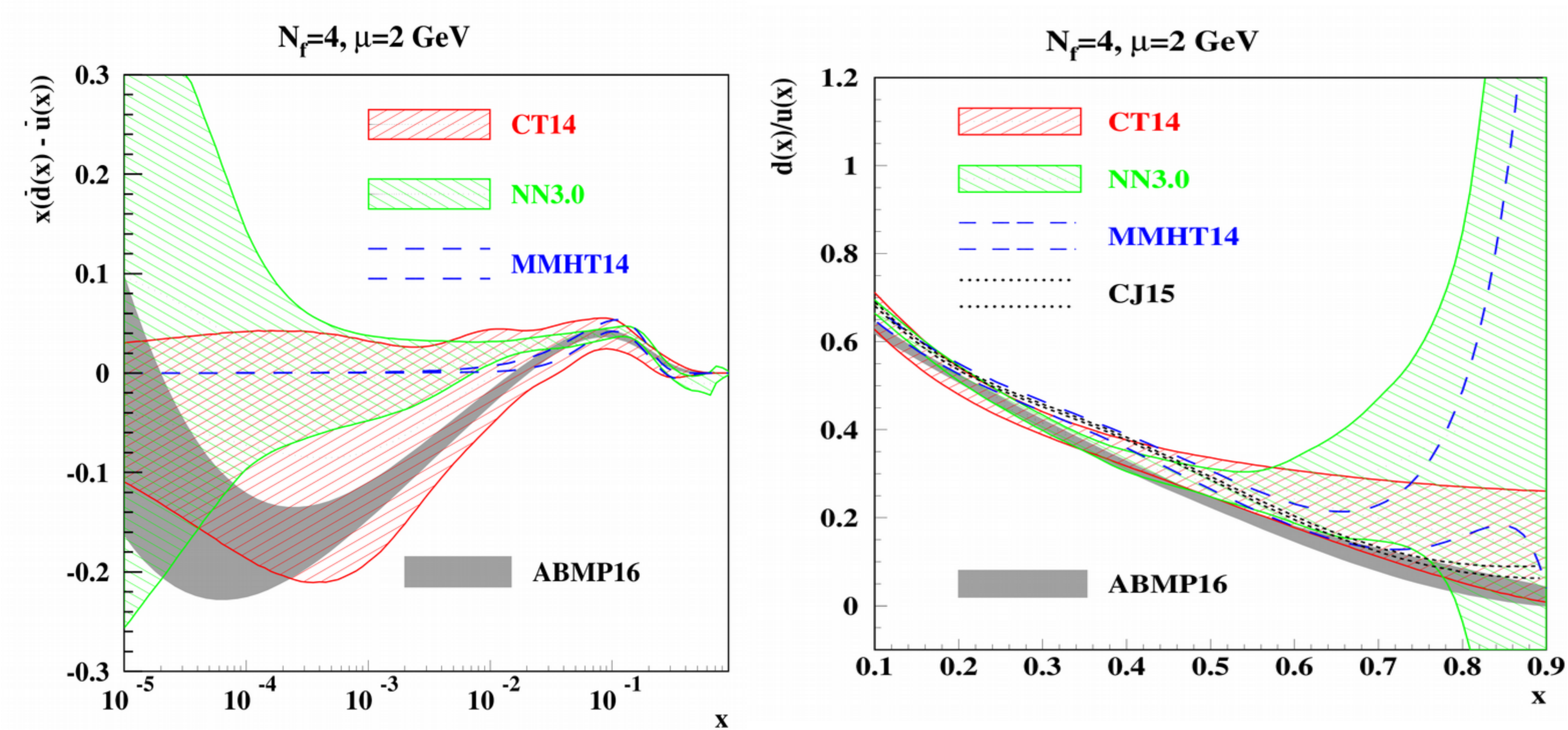


- Relaxed form of the sea iso-spin asymmetry I(x) at small x; Regge-like behaviour is recovered only at x~$10^{-6}$; at large x it is still defined by the phase-space constraint
- Big spread between different PDF sets, up to factor of 30 at large x → poor control of the BSM effects without constraints from the DY data
- Good constraint on the d/u ratio w/o deuteron data → independent extraction of the deuteron corrections

Accardi, Brady, Melnitchouk, Owens, Sato PRD 93, 114017 (2016)

# Impact of fixed-target deuteron data

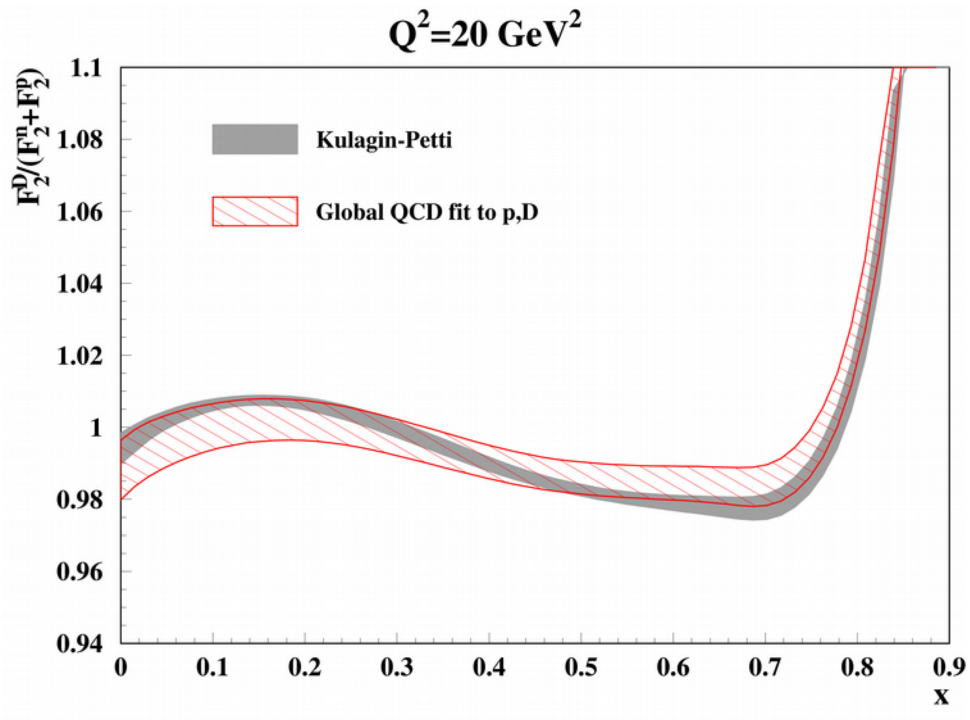


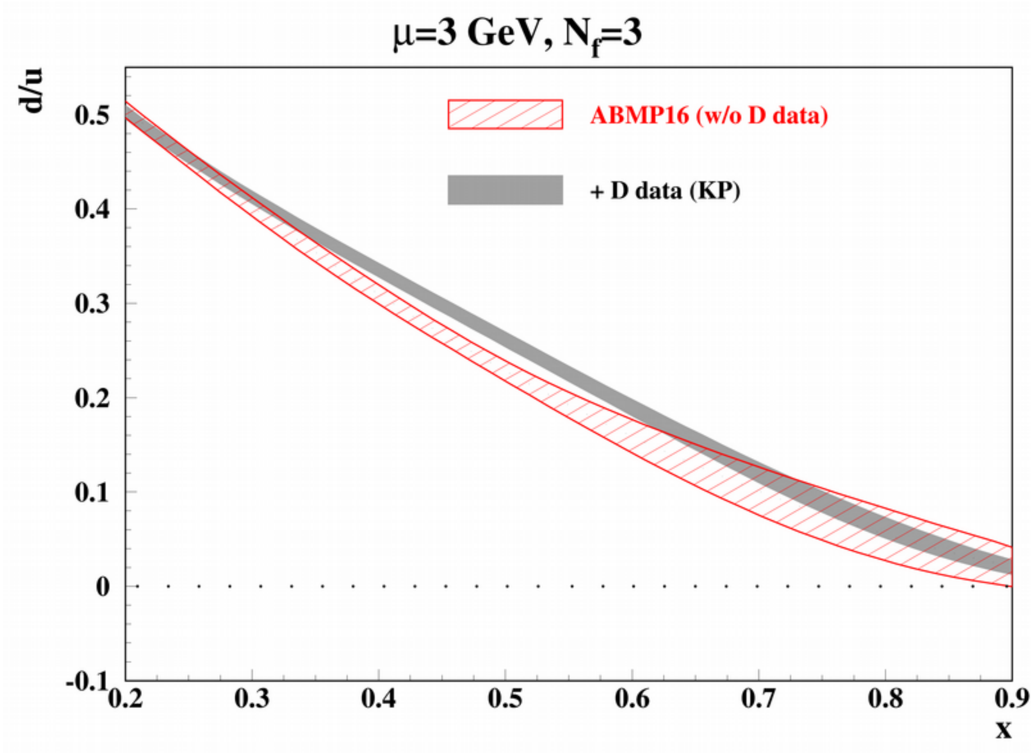


**sa, Kulagin, Petti PRD 96, 054005 (2017)**

*Nuclear corrections extracted from the deuteron data are in good agreement with the results obtained from the heavy-target ones ⇒ universality of the off-shell function is justified ⇒ application to the nucleon-nucleon collisions*

**Kulagin, Petti NPA 765, 126 (2006)**
**Kulagin, Petti PRD 94, 113013 (2016)**

*At large x the deuteron data further disentangle d- and u-distributions*

# CJ15 results on the d/u ratio

Accardi, Brady, Melnitchouk, Owens, Sato PRD 93, 114017 (2016)

- NLO PDF fit including Tevatron data on W-asymmetry
- value of d/u~0.07 at large x is obtained
- NLO FEWZ predictions with CJ15 PDFs miss data (limitation of the K-factor approach used by CJ15?)

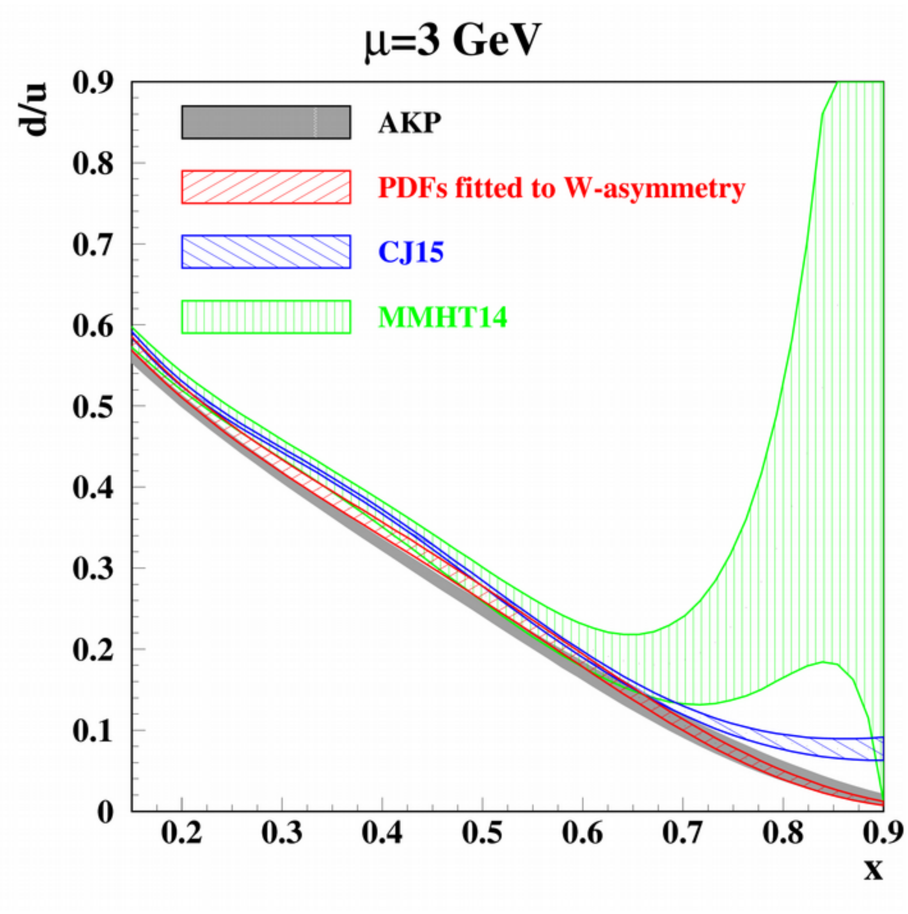


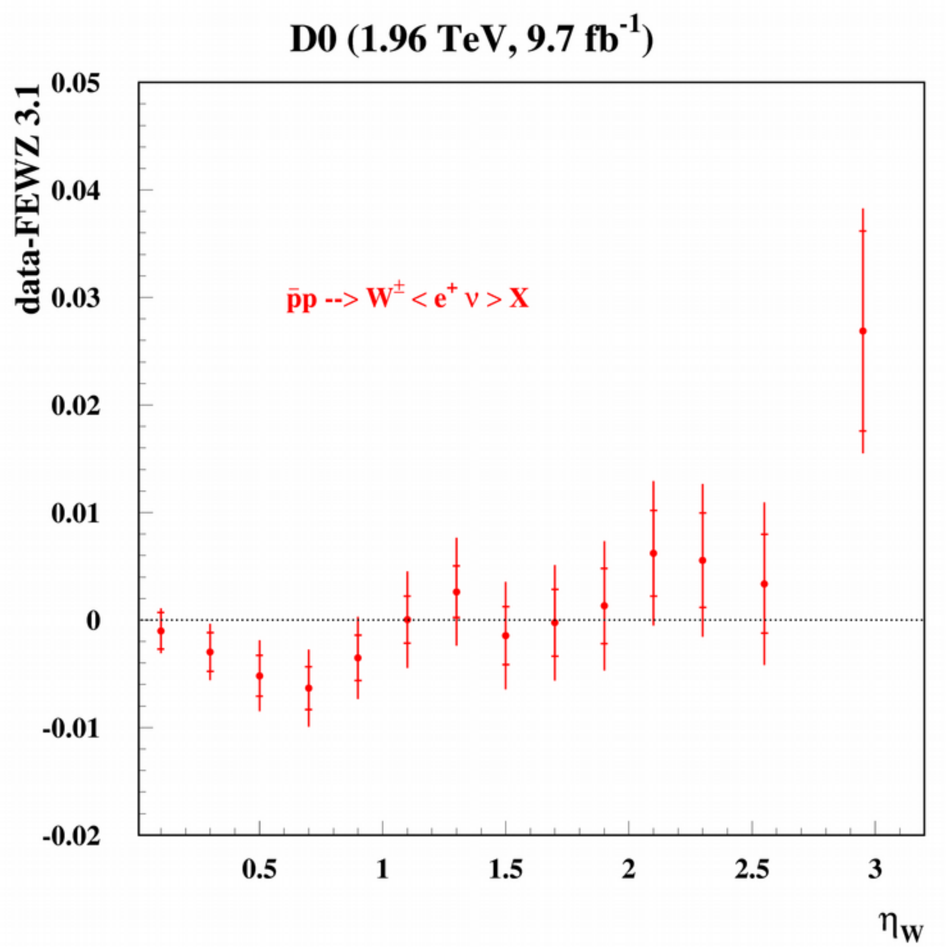

# Impact of the W-, Z-data in ABMP16 fit

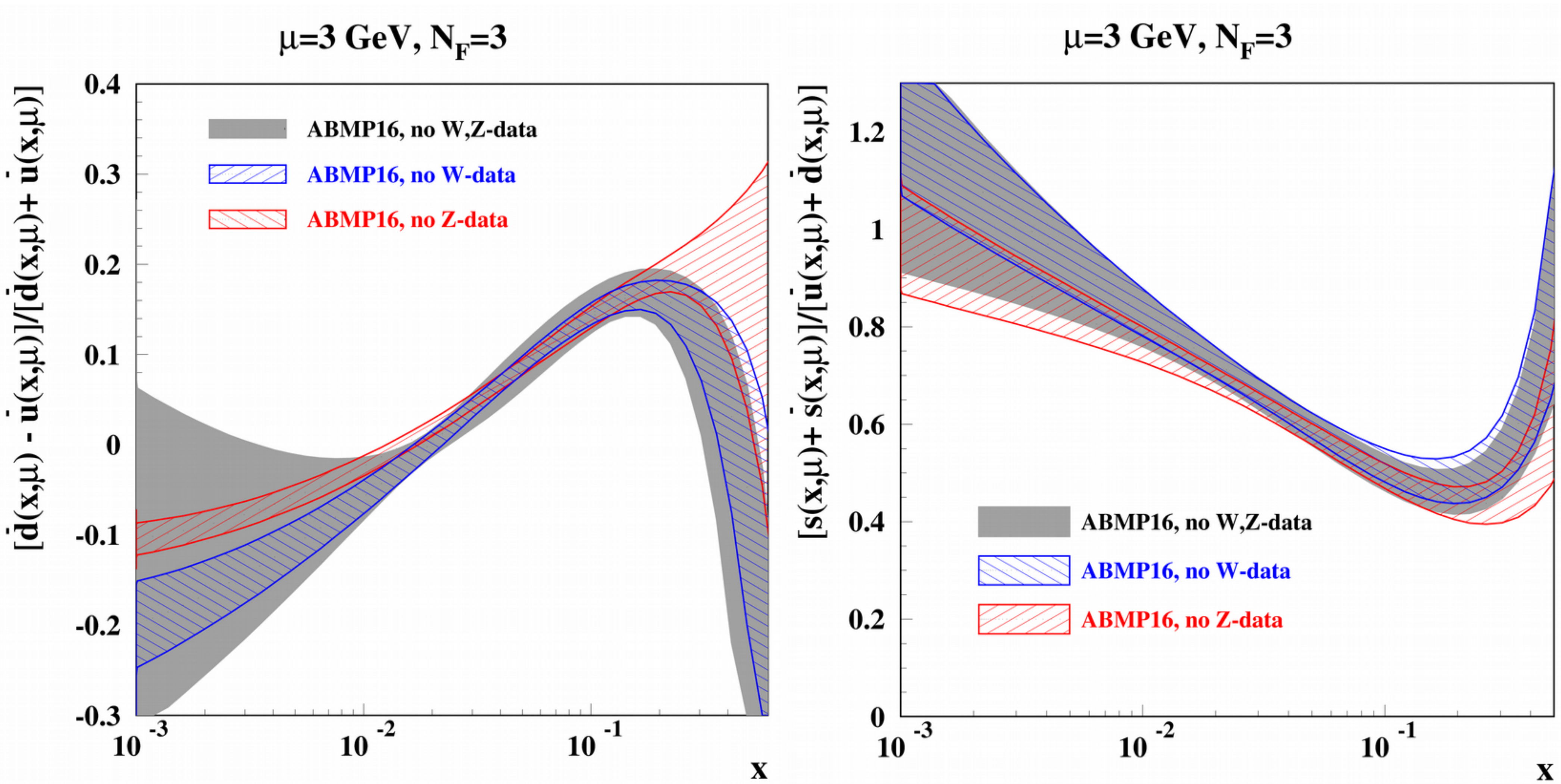


W-, Z-data really control quark disentangling at small x

# ATLAS strange enhancement

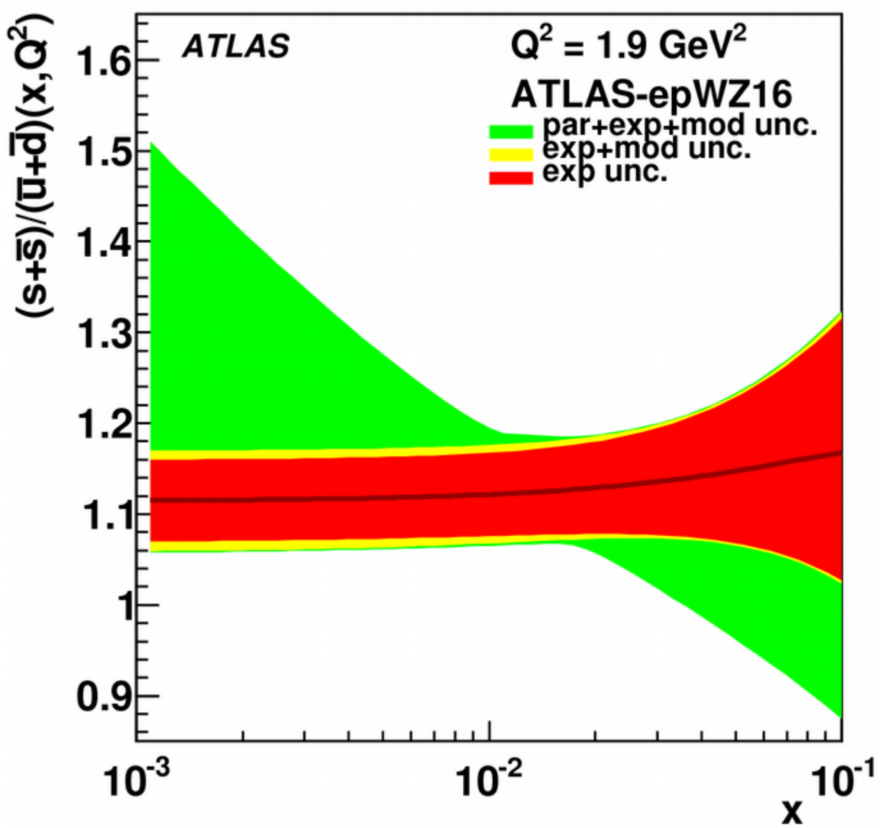


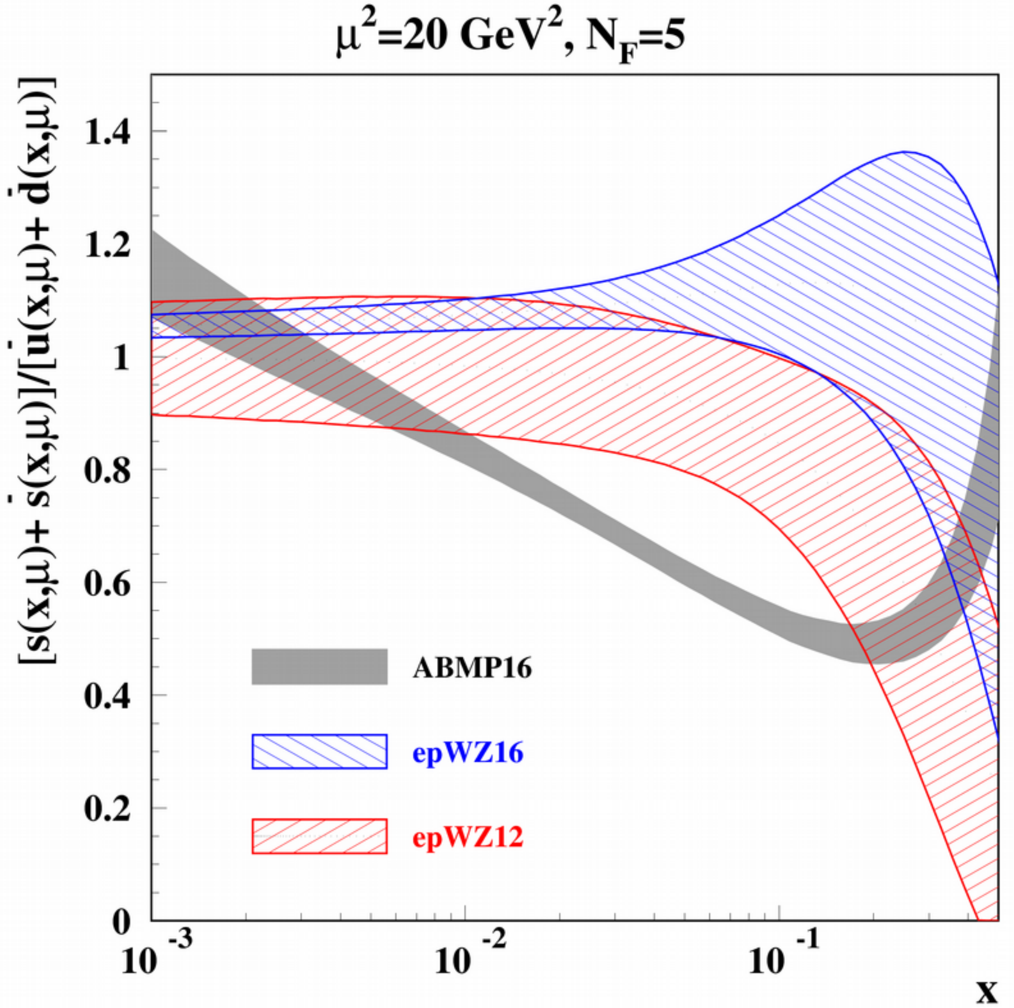


The epWZ16 strange-sea determined from analysis of the combined HERA-ATLAS data is enhanced as compared to other (earlier) determinations

ABM strange sea determination is in particular based on the dimuon neutrino-nucleon DIS production (NuTeV/CCFR and NOMAD) that gives a strange sea suppression ~0.5 at x~0.2

- *Disentangling d- and s- contribution?*
- *Impact of the nuclear corrections?*
- *…..?*

# Test fit (the PDF shape comparison)

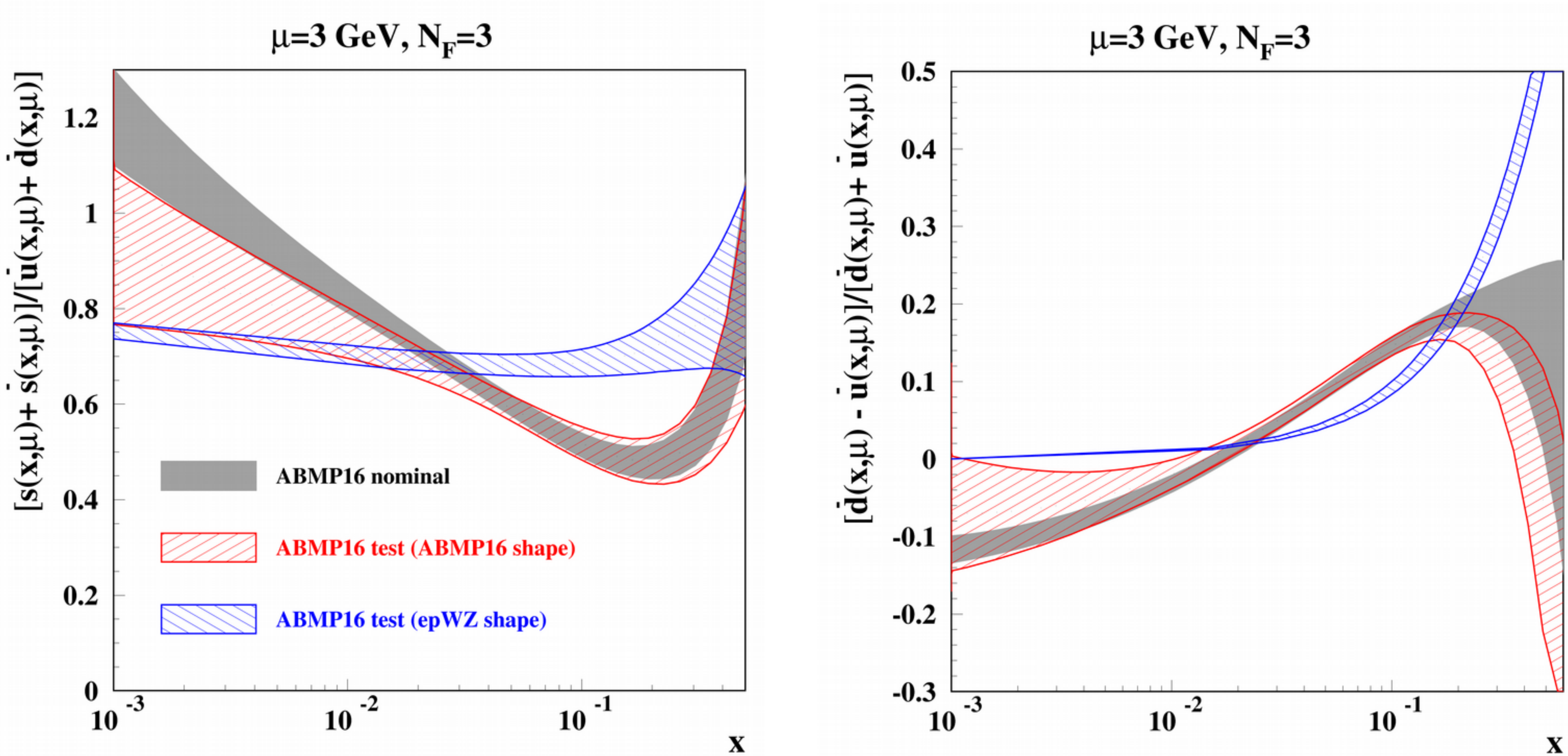


The data used in test fit: collider data discarded and replaced by the deuteron ones (fit is consistent with the nominal ABMP16 at x>0.01) **sa, Kulagin, Petti hep-ph/1704.00204**

*The strange sea is enhanced for the epWZ shape despite the ATLAS data are not used. However, the dimuon data description is not deteriorated: $\chi^2$=167 versus 161 for the ABMP shape ⇒ enhancement is achieved by the price of the d-quark sea suppression*

**sa, Blümlein, Caminada, Lipka, Lohwasser, Moch, Petti, Plačakytė PRD 91, 094002 (2015)**

# E866 data in the test fit

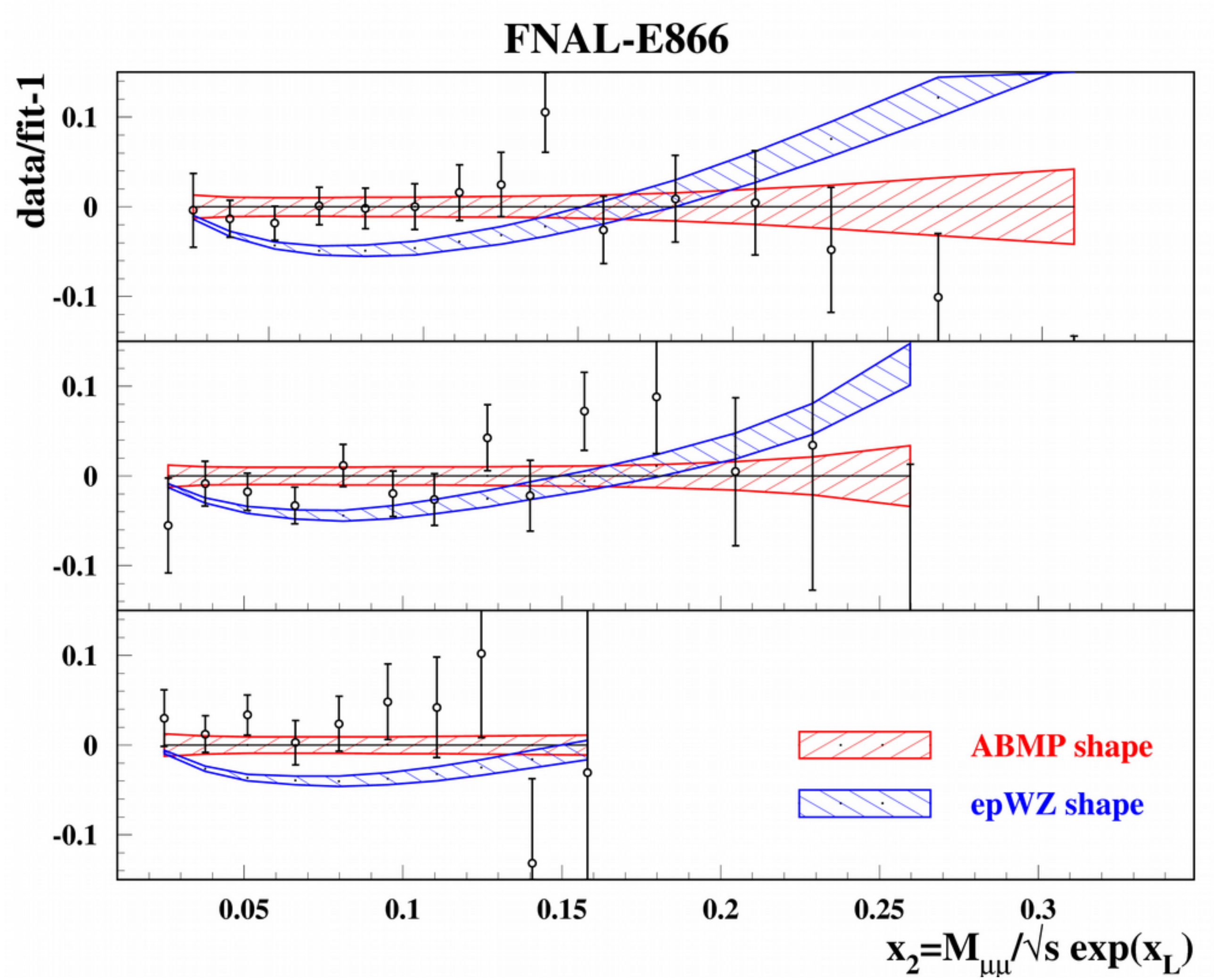


The E866 data on p/d DY cross sections are sensitive to the iso-spin sea asymmetry

*The epWZ shape does not allow to accommodate E866 data: $\chi^2$/NDP=96/39 versus 49/39 for the ABMP shape; the errors in epWZ predictions are suppressed at small x, evidently due to over-constrained PDF shape at small x*

# SeaQuest (FNAL-E906) prospects

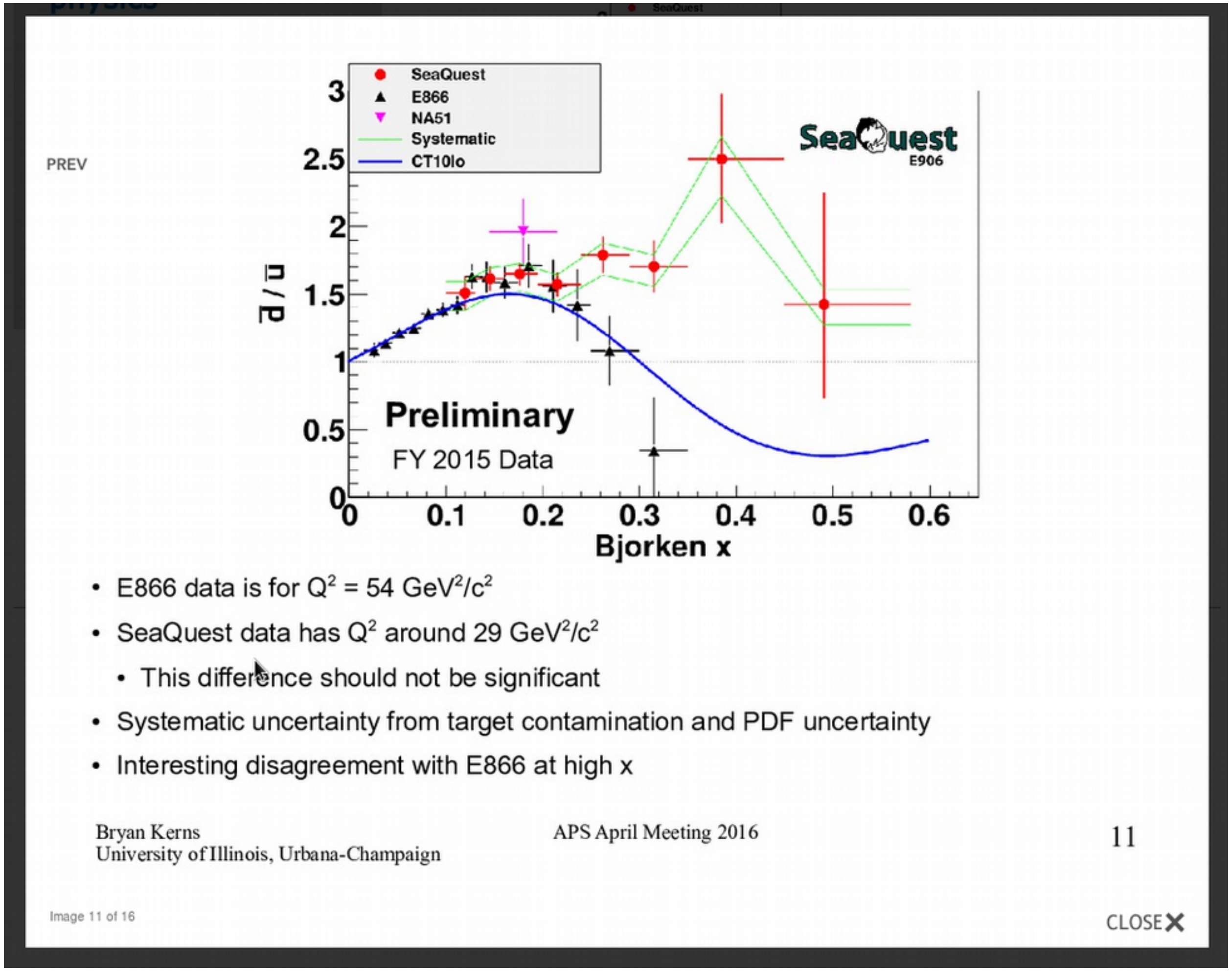


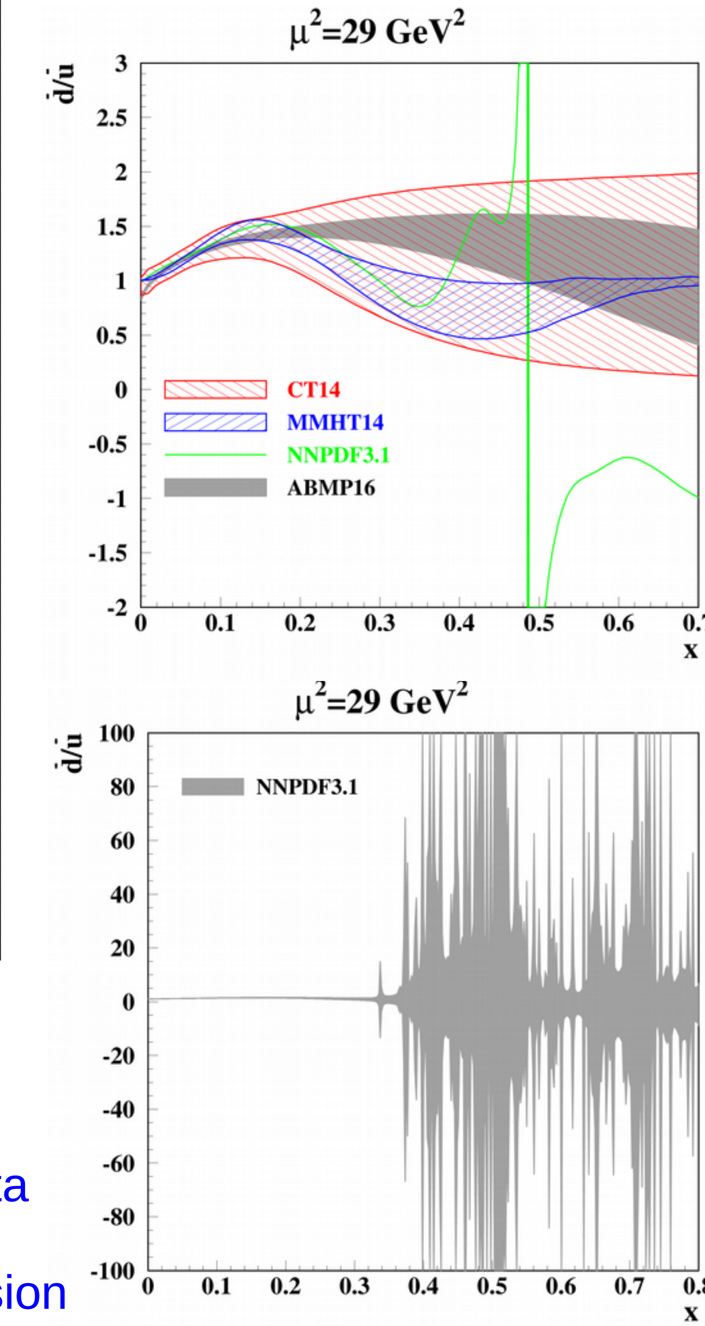


- E906 confirms the E866 results at x ~0.1 and continues the positive trend in the sea iso-spin asymmetry at bigger x
- The existing PDF sets can be consolidated with the E906 data
- HERMES/COMPASS data confirm the strangeness suppression

**Borsa, Sassot, Stratmann hep-ph/1708.01630**

# Impact of ATLAS data with flexible PDF shape

| | $\kappa_s(\mu^2=20\ \mathrm{GeV}^2)$ |
|---|---|
| HERA+ATLAS | 0.81(18) |
| HERA+ATLAS+E866 | 0.72(8) |
| ABMP16(incl. NOMAD) | 0.66(3) |

*$\kappa_s$ is integral strange sea suppression factor:*

$$\kappa_s(\mu^2) = \frac{\int_0^1 x[s(x,\mu^2)+\bar{s}(x,\mu^2)]dx}{\int_0^1 x[\bar{u}(x,\mu^2)+\bar{d}(x,\mu^2)]dx},$$

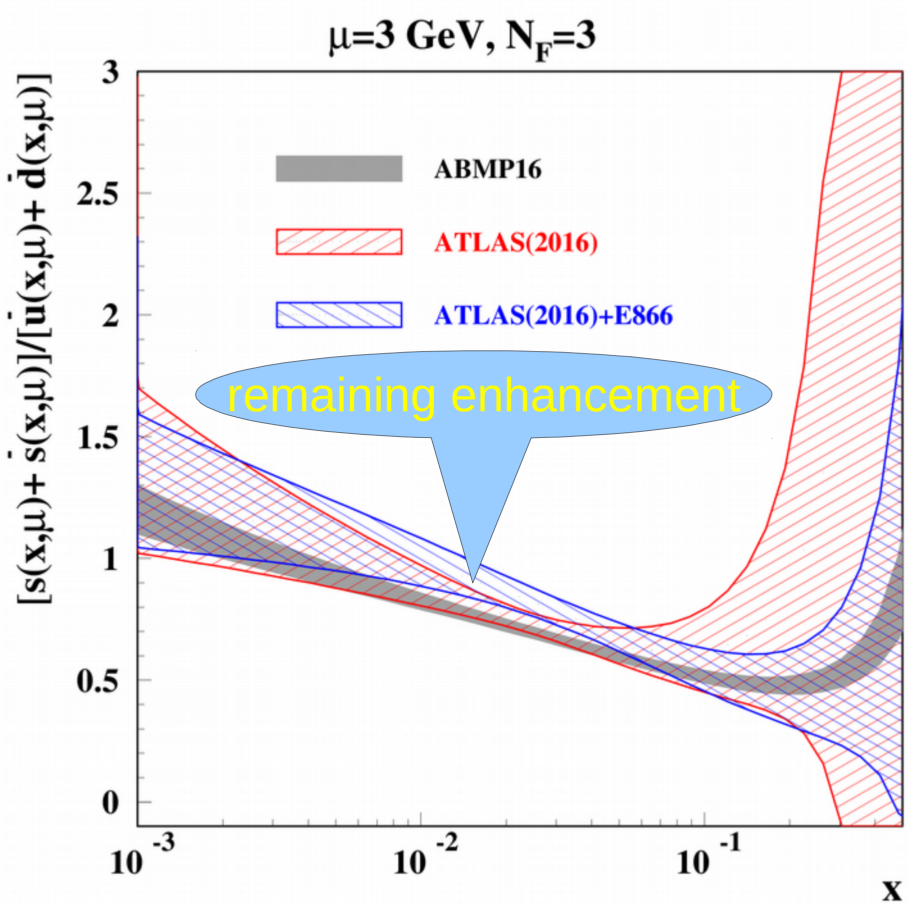


- For the flexible PDF shape the strangeness is in a broad agreement with the one extracted from the dimuon data
- The E866 data are consistent with the ATLAS(2016) set: $\chi^2$/NDP=48/39 and 40/34, respectively.

sa, Blümlein, Moch hep-ph/1708.01067

# Heavy-quark electro-production with FFN and VFN

- Only 3 light flavors appear in the initial state
- The dominant mechanism is photon-gluon fusion
- The coefficient functions are known up to the NLO

  **Witten NPB 104, 445 (1976)**
  **Laenen, Riemersma, Smith, van Neerven NPB 392, 162 (1993)**

- Involved high-order calculations:
  - NNLO terms due to threshold resummation

    **Laenen, Moch PRD 59, 034027 (1999)**
    **Lo Presti, Kawamura, Lo Presti, Moch, Vogt NPB 864, 399 (2012)**
    **sa, Moch, Blümlein PRD 96, 014011 (2017)**

  - limited set of the NNLO Mellin moments

    **Ablinger at al. NPB 844, 26 (2011)**
    **Bierenbaum, Blümlein, Klein NPB 829, 417 (2009)**
    **Ablinger et al. NPB 890, 48 (2014)**

- At large *Q* the leading-order coefficient → $\ln(Q/m_h)$ and may be quite big despite the suppression by factor of $\alpha_s$ and should be resummed

  **Shifman, Vainstein, Zakharov NPB 136, 157 (1978)**

→ a motivation to derive the VFN scheme matched to the FFNS (ACOT...., RT..., FONLL....)

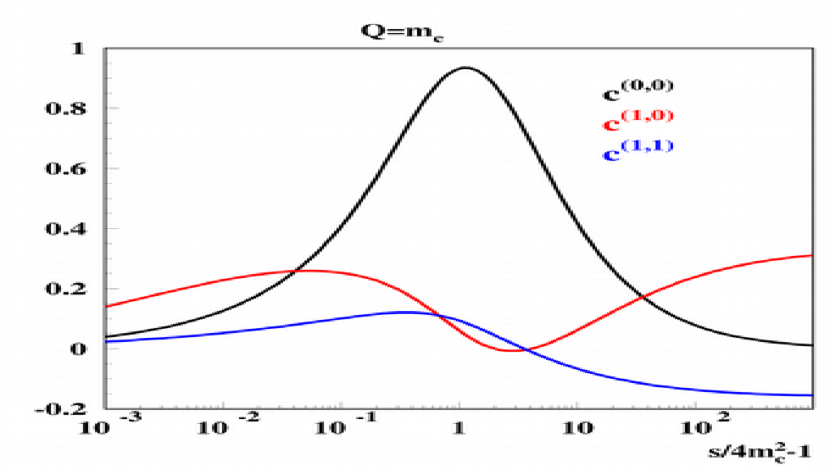


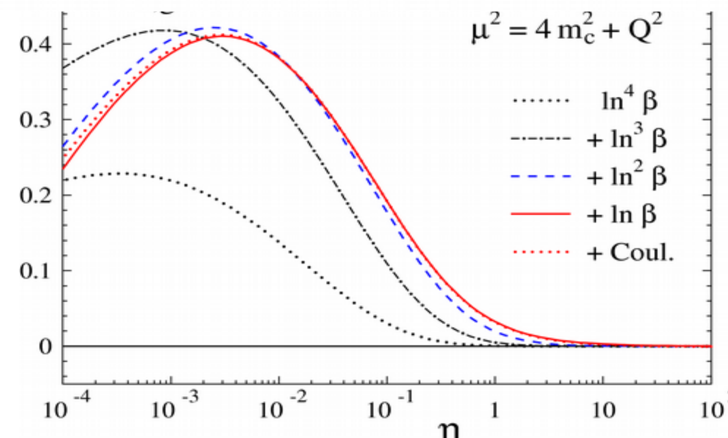


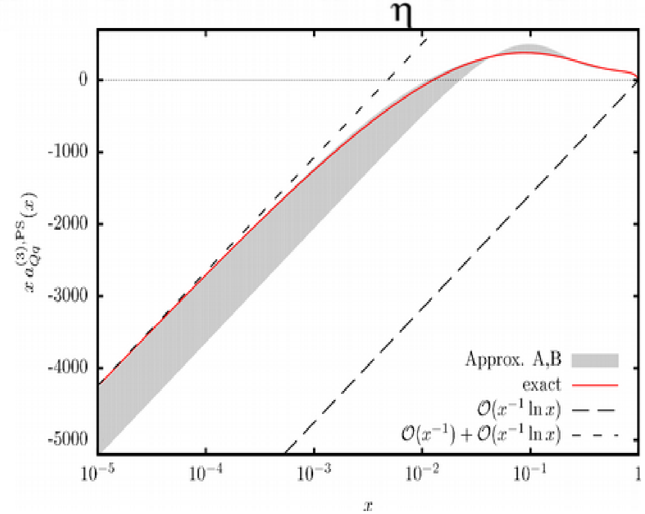

# FFN and VFN schemes

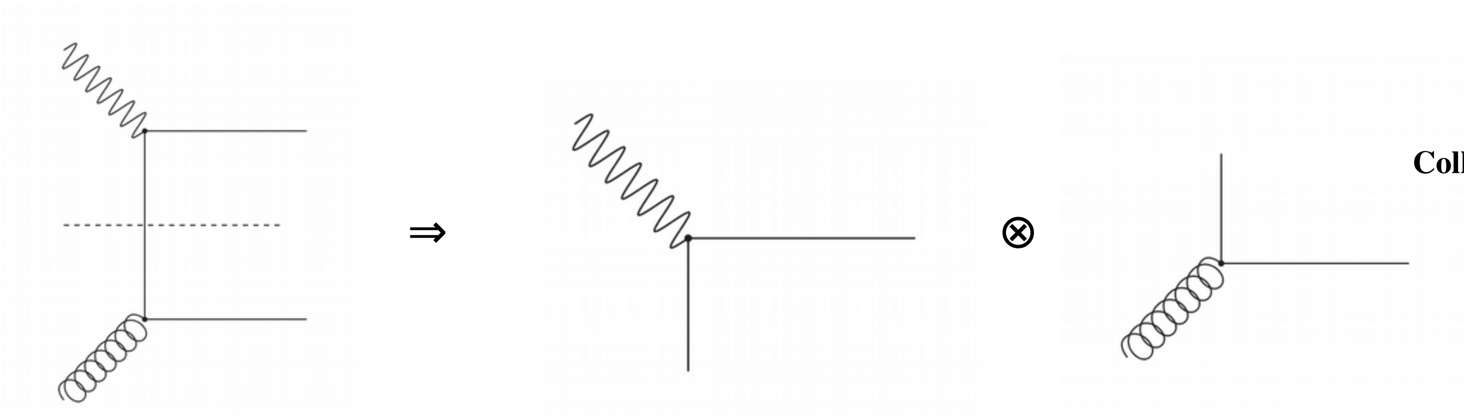

Collins, Tung NPB 278, 934 (1986)

$$H_{g,2}^{\mathrm{asymp}} = a_s(N_f) A_{hg}^{(1)}$$ Asymptotic 3-flavor coefficient function

LO

$$A_{ij}^{(1)}\left(z, \frac{m_h^2}{\mu^2}\right) = a_{ij}^{(1,1)}(z) \ln\left(\frac{\mu^2}{m_h^2}\right)$$ Massive operator matrix elements (OMEs)

$$h^{(1)}(x,\mu^2) = a_s(N_f+1,\mu^2)\left[A_{hg}^{(1)}\left(\frac{m_h^2}{\mu^2}\right) \otimes G^{(2)}\left(N_f,\mu^2\right)\right](x)$$ Matching condition for the heavy-quark PDFs

$$F_{g,2}^{\mathrm{asymp}} = e_h^2 x h^{(1)}(x,\mu^2)$$

NLO ...

Buza, Matiounine, Smith, van Neerven EPJC 1, 301 (1998)

$$A_{ij}^{(2)}\left(z, \frac{m_h^2}{\mu^2}\right) = a_{ij}^{(2,2)}(z) \ln^2\left(\frac{\mu^2}{m_h^2}\right) + a_{ij}^{(2,1)}(z) \ln\left(\frac{\mu^2}{m_h^2}\right) + a_{ij}^{(2,0)}(z)$$

NNLO

Blümlein, et al., work in progress

- The VFN scheme works well at $\mu \gg m_h$ (W,Z,t-quark production,....)
- Problematic for DIS ⇒ additional modeling of power-like terms required (ACOT, BMSN, FONLL, RT....)

# Modeling NNLO massive coefficients

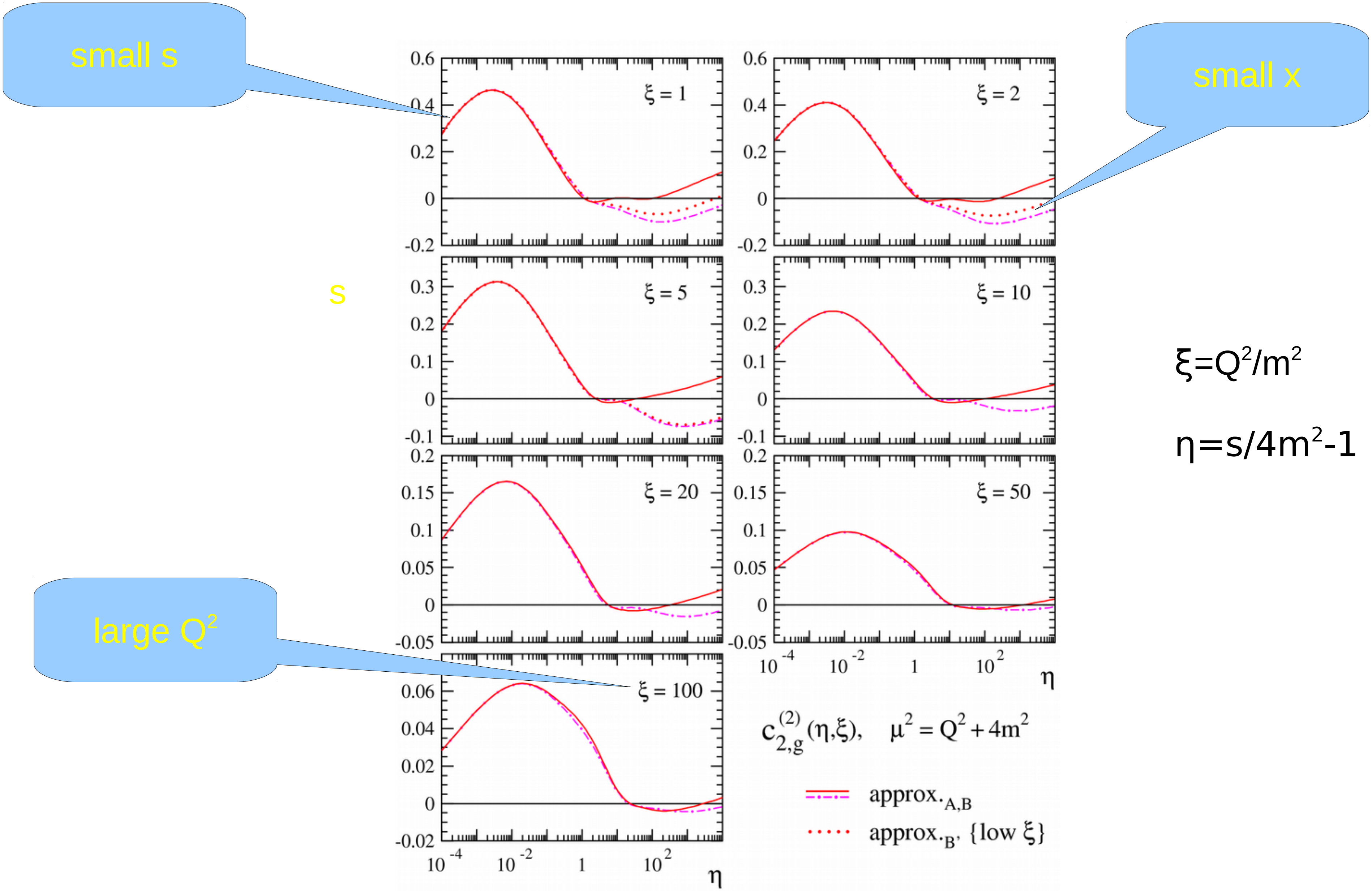


$\xi = Q^2/m^2$

$\eta = s/4m^2 - 1$

Combination of the threshold corrections (small s), high-energy limit (small x), and the NNLO massive OMEs (large $Q^2$)

**Kawamura, Lo Presti, Moch, Vogt NPB 864, 399 (2012)**

# Recent progress in massive DIS coefficients

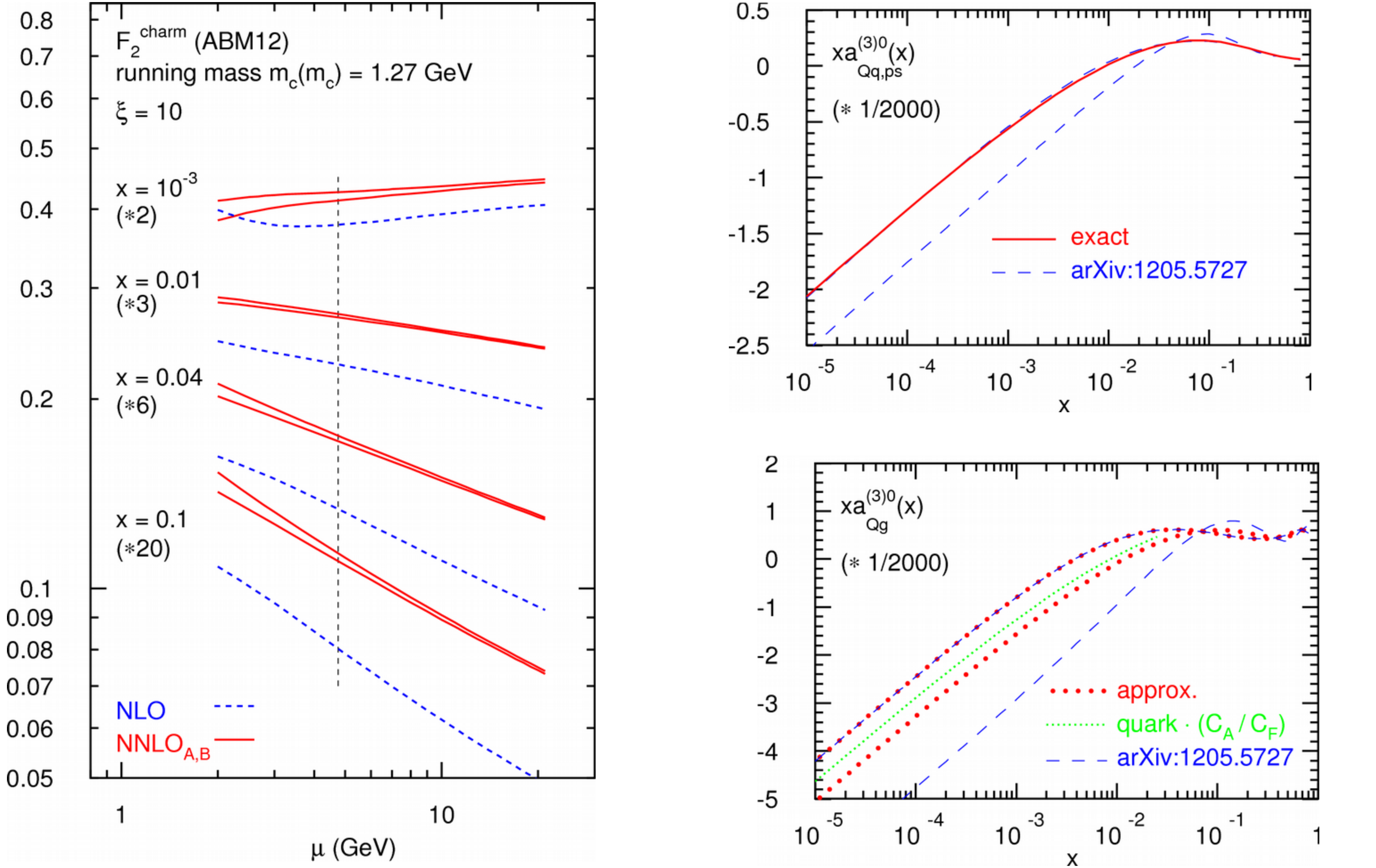


Update with the pure singlet massive OMEs → improved theoretical uncertainties

sa, Moch, Blümlein PRD 96, 014011 (2017)

# Factorization scheme benchmarking

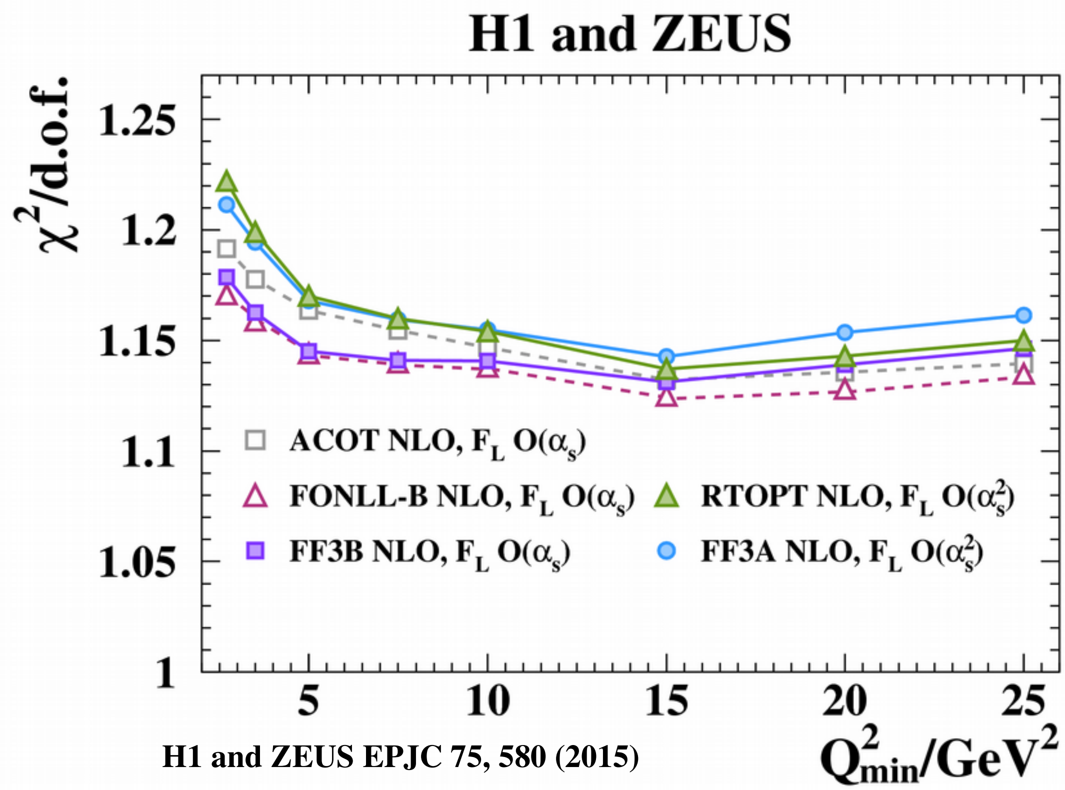


H1 and ZEUS EPJC 75, 580 (2015)

- Data allow to discriminate factorization schemes
- FFN scheme works very well in case of correct setting (running mass definition and correct value of $m_c$) → no traces of big logs due to resummation

| $x_{min}$ | $x_{max}$ | $Q^2_{min}$ (GeV) | $Q^2_{max}$ (GeV) | $\Delta\chi^2$ (DIS) | $N^{DIS}_{dat}$ | $\Delta\chi^2$ (HERA-I) | $N^{hera-I}_{dat}$ |
|---|---|---|---|---|---|---|---|
| $4 \cdot 10^{-5}$ | 1 | 3 | $10^6$ | 72.2 | 2936 | 77.1 | 592 |
| $4 \cdot 10^{-5}$ | 0.1 | 3 | $10^6$ | 87.1 | 1055 | 67.8 | 405 |
| $4 \cdot 10^{-5}$ | 0.01 | 3 | $10^6$ | 40.9 | 422 | 17.8 | 202 |
| $4 \cdot 10^{-5}$ | 1 | 10 | $10^6$ | 53.6 | 2109 | 76.4 | 537 |
| $4 \cdot 10^{-5}$ | 1 | 100 | $10^6$ | 91.4 | 620 | 97.7 | 412 |
| $4 \cdot 10^{-5}$ | 0.1 | 10 | $10^6$ | 84.9 | 583 | 67.4 | 350 |
| $4 \cdot 10^{-5}$ | 0.1 | 100 | $10^6$ | 87.7 | 321 | 87.1 | 227 |

*"We conclude that the FFN fit is actually based on a less precise theory, in that it does not include full resummation of the contribution of heavy quarks to perturbative PDF evolution, and thus provides a less accurate description of the data"*

NNPDF PLB 723, 330(2013)

# Running mass in DIS

The pole mass is defined for the free (*unobserved*) quarks as a the QCD Lagrangian parameter and is commonly used in the QCD calculations

$$\mathcal{L} = -\frac{1}{4} F_{\mu\nu} F^{\mu\nu} + \sum_{\text{flavors}} \bar{q}\,(\mathrm{i}\not{D} - m_q)\,q$$

$$\not{p} - m_q - \Sigma(p, m_q)\Big|_{p^2 = m_q^2}$$

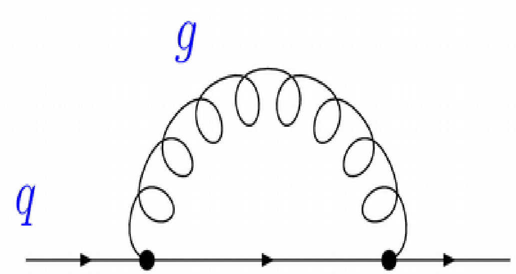


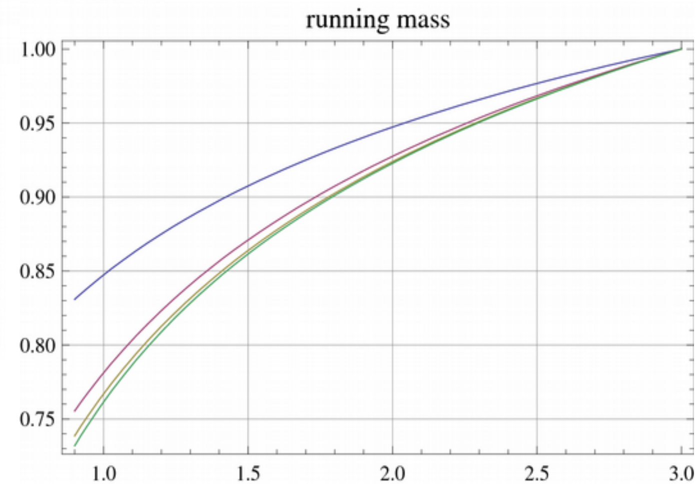


The quantum corrections due to the self-energy loop Integrals receive contribution down to scale of $O(\Lambda_{QCD})$

→ sensitivity to the high order corrections, particularly at the production threshold

$$\mu^2 \frac{d}{d\mu^2} m(\mu) = \gamma(\alpha_s) m(\mu)$$

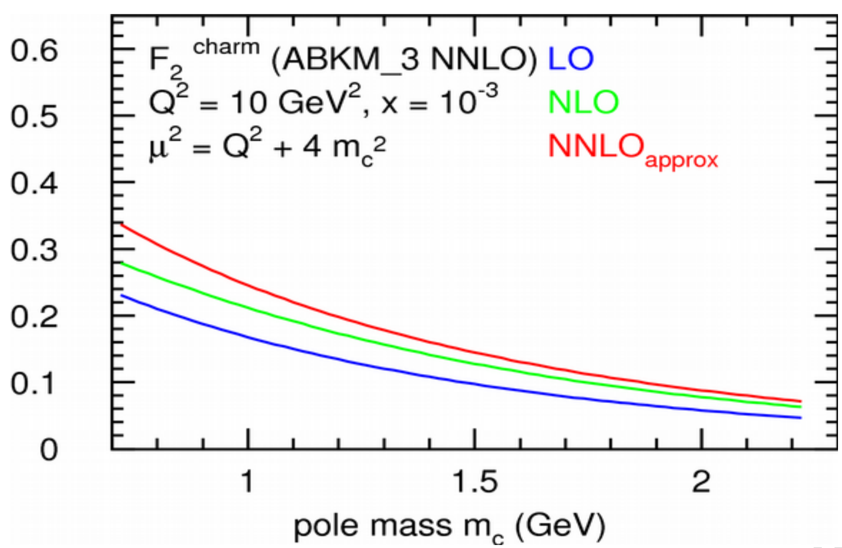


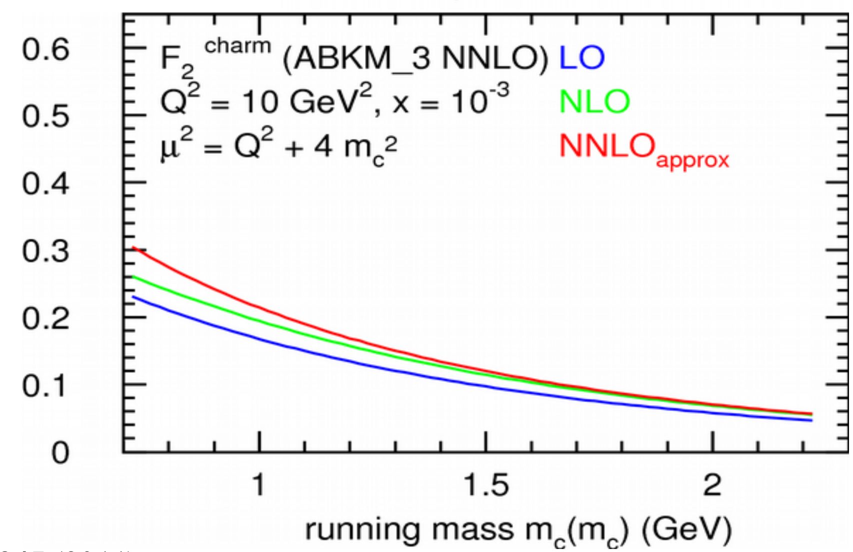


**sa, Moch PLB 699, 345 (2011)**

# c-quark mass in the CMVFN schemes

The values of pole mass $m_c$ used by different groups and preferred by the PDF fits are systematically lower than the PDG value

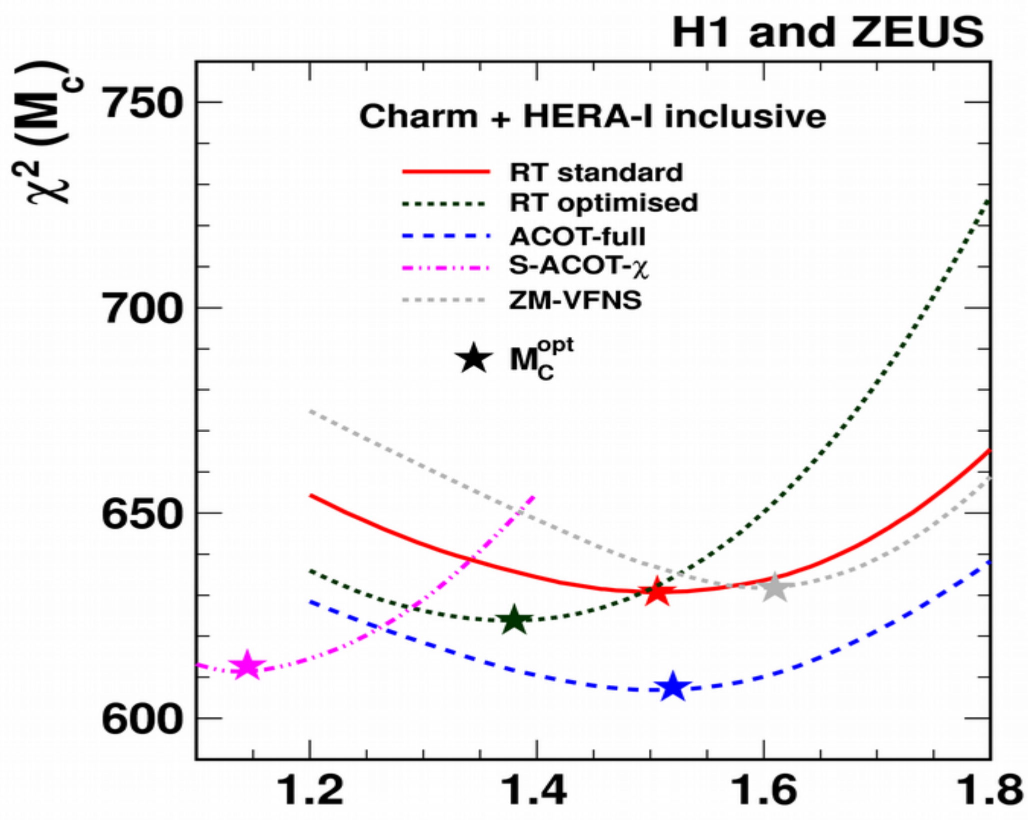


H1/ZEUS PLB 718, 550 (2012) $M_c$ [GeV]

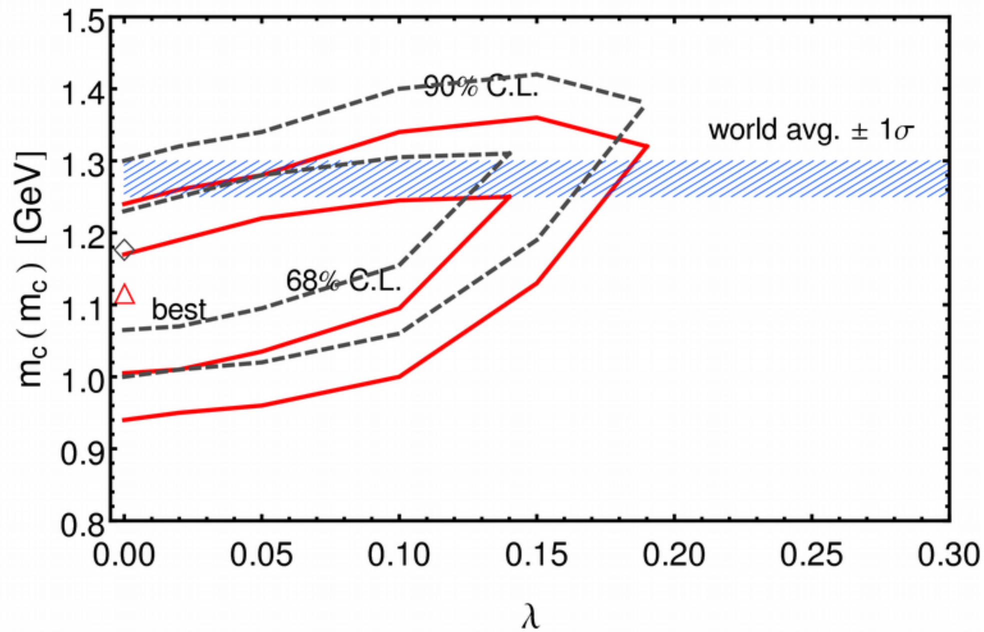


$m_c(m_c)$=1.19+0.08-0.15 GeV ACOT....

**Gao, Guzzi, Nadolsky EPJC 73, 2541 (2013)**

$m_c(m_c)$=1.34+0.04-0.01 GeV FONLL

**Bertone et. al JHEP 1608, 050 (2016)**

Wide spread of the $m_c$ obtained in different version of the GMVFN schemes → quantitative illustration of the GMVFNS uncertainties

# HERA charm data and $m_c(m_c)$

H1/ZEUS ZPC 73, 2311 (2013)

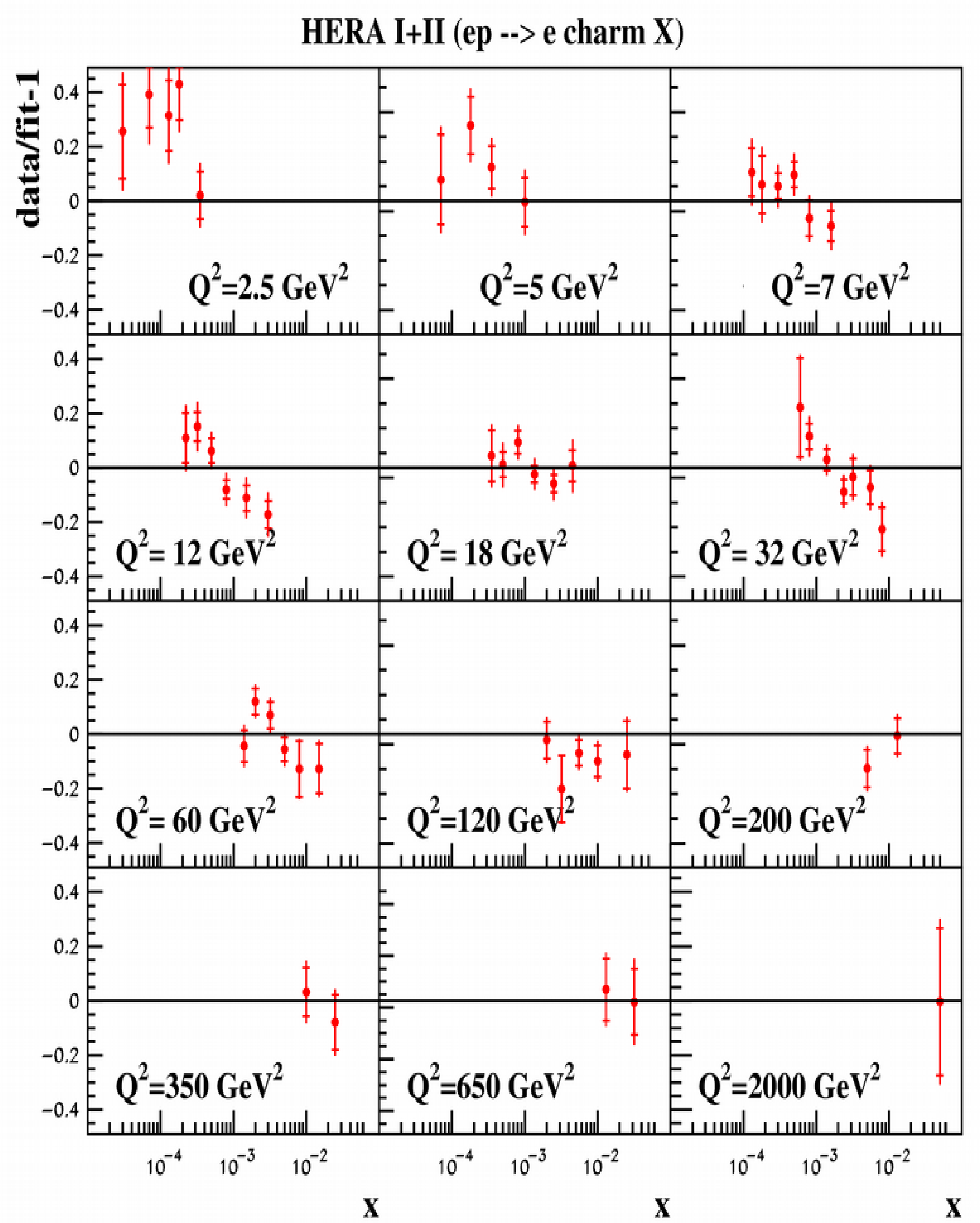


$m_c(m_c)$=1.246±0.023 (h.o.) GeV NNLO

Kiyo, Mishima, Sumino PLB 752, 122 (2016)

$X^2$/NDP=66/52

$m_c(m_c)$=1.252±0.018(exp.)-0.01(th.) GeV

ABMP16

$m_c(m_c)$=1.24±0.03(exp.) GeV ABM12

$m_c$(pole)~1.9 GeV (NNLO)

Marquard et al. PRL 114, 142002 (2015)

- RT optimal
  $X^2$/NDP=82/52 NNLO
  $m_c$(pole)=1.25 GeV
  MMHT14 EPJC 75, 204 (2015)

- S-ACOT-χ
  $X^2$/NDP=59/47 NNLO
  $m_c$(pole)=1.3 GeV
  CT14 PRD 93, 033006 (2016)

- F0NLL
  $X^2$/NDP=60/47 NNLO
  $m_c$(pole)=1.275 GeV
  NNPDF3.0 JHEP 504, 040 (2015)

- F0NLL
  $X^2$/NDP=54/37 NNLO
  $m_c$(pole)=1.51 GeV, intrinsic charm included
  NNPDF3.1 hep-ph/1706.00428

Accardi, et al. EPJC 76, 471 (2016)

# Intrinsic charm: pitfalls

- No mass singularities for massive partons ⇒ collinear QCD evolution does not work
- The mass singularities ~$\ln(\mu/m_h)$ appear at $\mu \gg m_h$ and the evolution restores. New charm(bottom) quark distribution may be introduced, however, extrapolation to smaller scales is still problematic
- Intrinsic charm is often introduced within the VFN framework ⇒ interplay with the "standard" VFN modeling of power-like terms
- Original formulation of the intrinsic charm implies its power-like behavior;

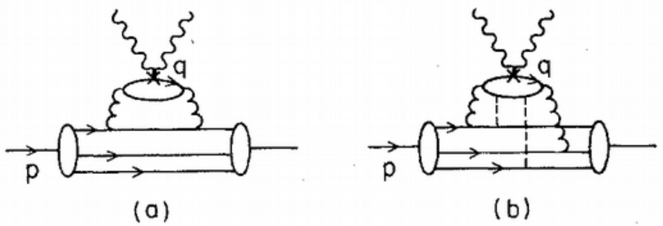


FIG. 7. (a) Example with contribution to the deep-inelastic structure functions from an extrinsic quark $q$; (b) from an intrinsic quark $q$.

**Brodsky, Peterson, Sakai PRD 23, 2745 (1981)**

strong constraint on such terms was obtained from analysis of the EMC data on charm production **Jimenez-Delgado, Hobbs, Londergan, Melnitchouk PRL 114, 082002 (2015)**

# Intrinsic charm in the CT and NNPDF fits

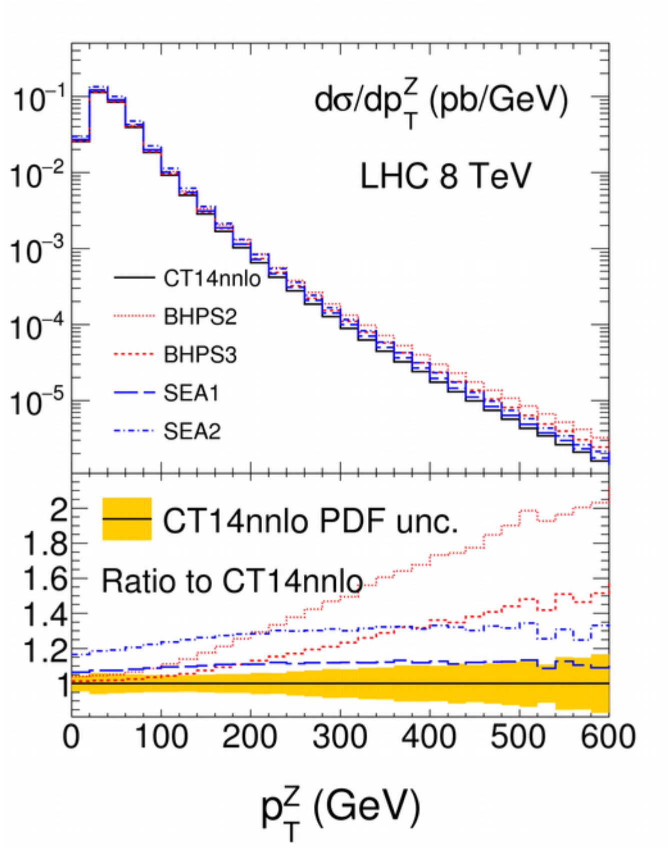


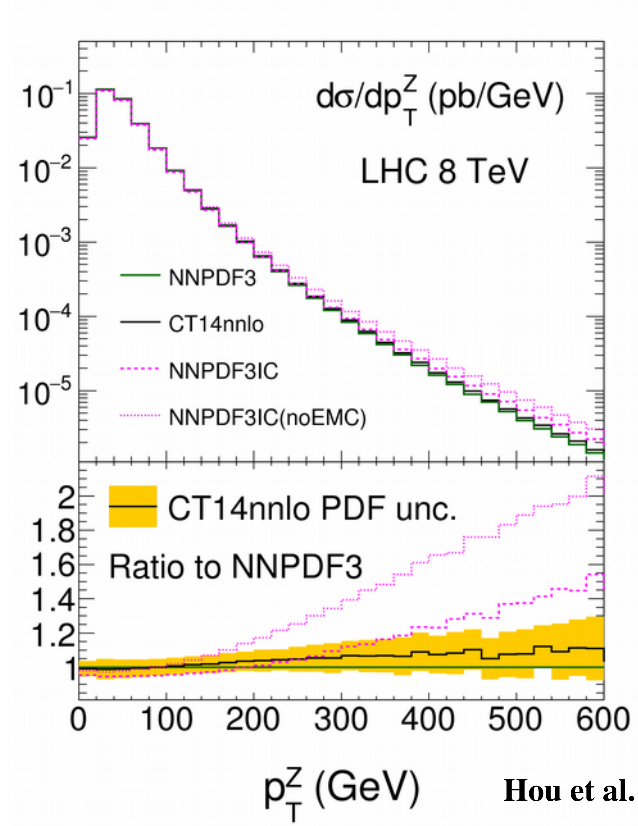


**Hou et al. hep-ph/1707.00657**

- The intrinsic-charm (IC) component is evolved starting from the small scale with the collinear DGLAP
- The value of $m_c$(pole)=1.31 (CT) and 1.51(NNPDF) GeV is used
- Several IC shapes are considered by CT: BHPS, SEA,…; free form by NNPDF
- An agreement with the Z+charm LHC data might be improved

**NNPDF hep-ph/1706.00428**

# Summary

We have steady improvement in the quark PDFs' determination

- disentangling d- and u-quark distributions at small x: impact of the LHC DY data in combination with the DIS ones

- improvement in the large-x d- and u-quark distributions: impact of the forward LHC and Tevatron data; deuteron data provided further constraints

- somewhat enhanced strange distribution at small x, however, the large-x enhancement reported by ATLAS seems to be an artefact of the PDF shape used

The HERA inclusive and semi-inclusive data allow to distinguish between the FFN and VFN factorization schemes in DIS. The FFN scheme provides nice agreement with existing data and

$$m_c(m_c)=1.252\pm0.018(\text{exp.})-0.01(\text{th.})\ \text{GeV},$$

in a good agreement with other determinations.

Intrinsic charm provides a new window for phenomenology, however, solid theoretical footing is still needed.

# EXTRAS

# HERA bottom data and $m_b(m_b)$

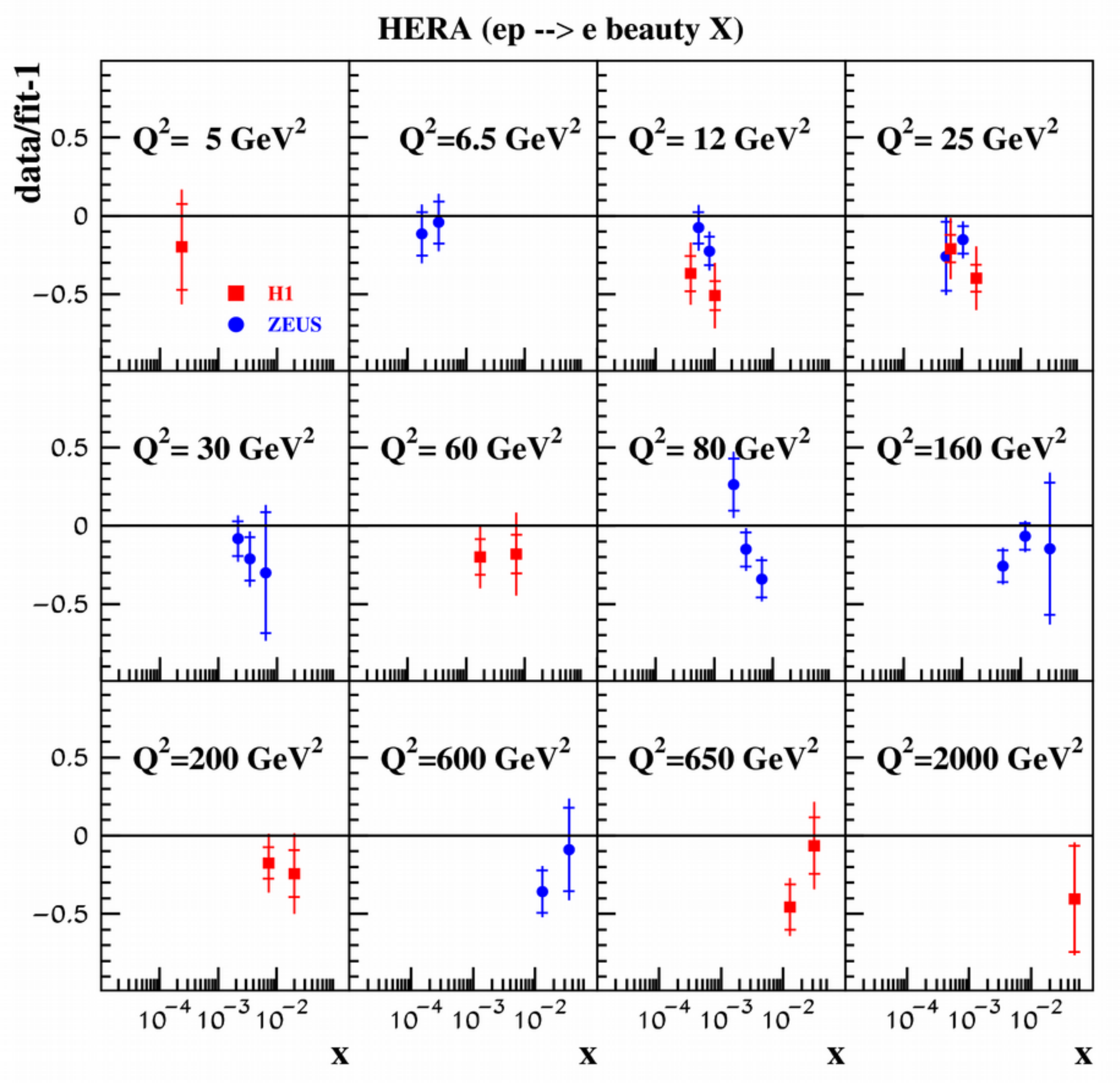


**ZEUS JHEP 1409, 127 (2014)**

$\chi^2$/NDP=16/17

**H1 EPJC 65, 89 (2010)**

$\chi^2$/NDP=5/12

$m_b(m_b)$=3.83±0.12(exp.)-0.1(th.) GeV

# NNLO DY corrections in the fit

The existing NNLO codes (DYNNLO, FEWZ) are quite time-consuming → fast tools are employed (FASTNLO, Applgrid,.....)

- the corrections for certain basis of PDFs are stored in the grid
- the fitted PDFs are expanded over the basis
- the NNLO c.s. in the PDF fit is calculated as a combination of expansion coefficients with the pre-prepared grids

The general PDF basis is not necessary since the PDFs are already constrained by the data, which do not require involved computations → *use as a PDF basis the eigenvalue PDF sets obtained in the earlier version of the fit*

$\mathbf{P_0} \pm \Delta\mathbf{P}_0$ – vector of PDF parameters with errors obtained in the earlier fit
**E** – error matrix
**P** – current value of the PDF parameters in the fit

- store the DY NNLO c.s. for all PDF sets defined by the eigenvectors of **E**
- the variation of the fitted PDF parameters ($\mathbf{P} - \mathbf{P}_0$) is transformed into this eigenvector basis
- the NNLO c.s. in the PDF fit is calculated as a combination of transformed ($\mathbf{P} - \mathbf{P}_0$) with the stored eigenvector values

# DY at large rapidity

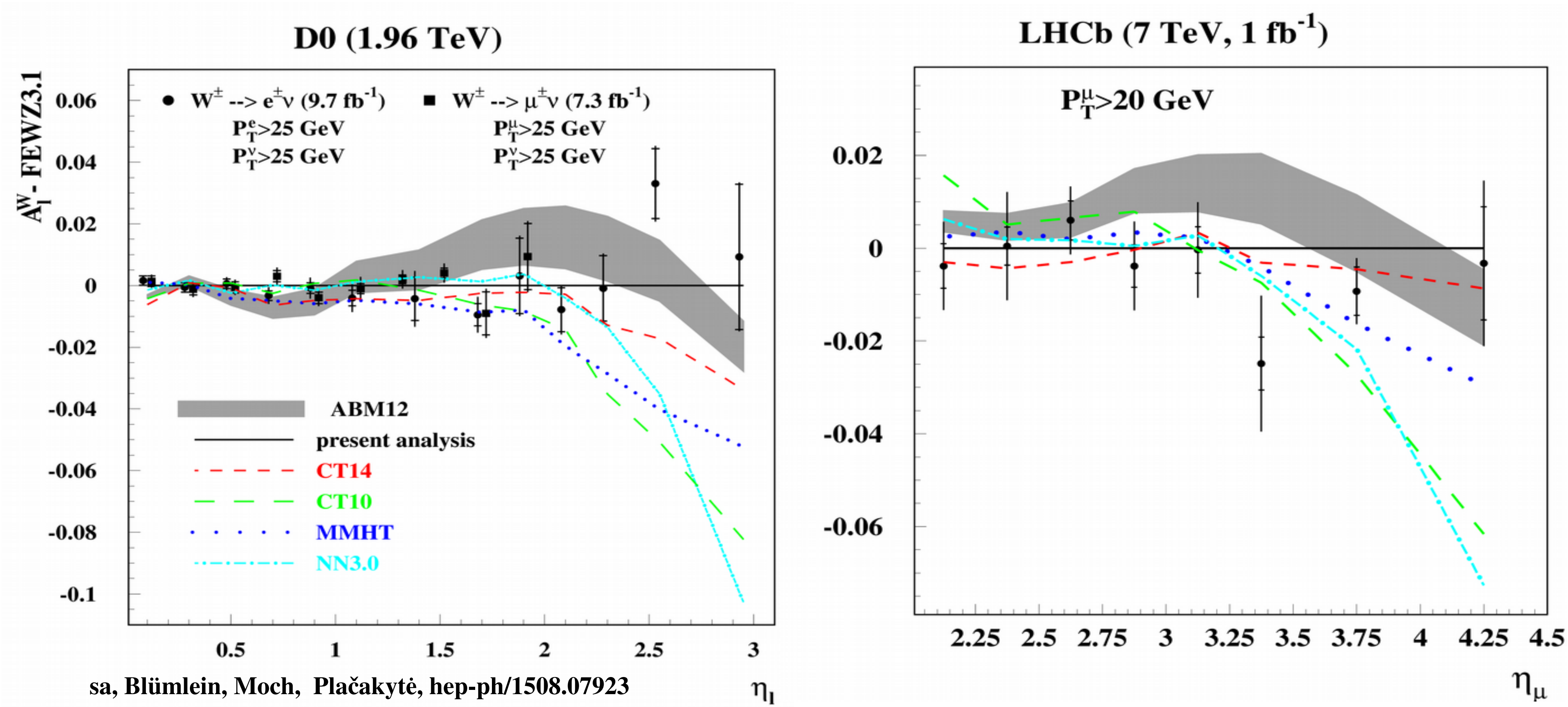


- The data can be evidently used for consolidation of the PDFs, however, unification of the theoretical accuracy is also needed

| ABM | CT | MMHT | NNPDF |
|---|---|---|---|
| Interpolation of accurate NNLO grid (a la FASTNLO) | NNLL (ResBos) | NLO + NNLO K-factor | NLO + NNLO C-factors (y-dependent K-factors) |

| PDF sets | $m_c$ [GeV] | $m_c$ renorm. scheme | theory method ($F_2^c$ scheme) | theory accuracy for heavy quark DIS Wilson coeff. | $\chi^2$/NDP for HERA data [127] with xFitter [128, 129] | |
|---|---|---|---|---|---|---|
| ABM12 [2] [a] | $1.24 \,^{+0.05}_{-0.03}$ | $\overline{\text{MS}}$ $m_c(m_c)$ | FFNS ($n_f = 3$) | $\text{NNLO}_{\text{approx}}$ | 65/52 | 66/52 |
| CJ15 [1] | 1.3 | $m_c^{\text{pole}}$ | SACOT [122] | NLO | 117/52 | 117/52 |
| CT14 [3] [b] | | | | | | |
| (NLO) | 1.3 | $m_c^{\text{pole}}$ | SACOT($\chi$) [123] | NLO | 51/47 | 70/47 |
| (NNLO) | 1.3 | $m_c^{\text{pole}}$ | SACOT($\chi$) [123] | NLO | 64/47 | 130/47 |
| HERAPDF2.0 [4] | | | | | | |
| (NLO) | 1.47 | $m_c^{\text{pole}}$ | RT optimal [125] | NLO | 67/52 | 67/52 |
| (NNLO) | 1.43 | $m_c^{\text{pole}}$ | RT optimal [125] | NLO | 62/52 | 62/52 |
| JR14 [5] [c] | 1.3 | $\overline{\text{MS}}$ $m_c(m_c)$ | FFNS ($n_f = 3$) | $\text{NNLO}_{\text{approx}}$ | 62/52 | 62/52 |
| MMHT14 [6] | | | | | | |
| (NLO) | 1.4 | $m_c^{\text{pole}}$ | RT optimal [125] | NLO | 72/52 | 78/52 |
| (NNLO) | 1.4 | $m_c^{\text{pole}}$ | RT optimal [125] | NLO | 71/52 | 83/52 |
| NNPDF3.0 [7] | | | | | | |
| (NLO) | 1.275 | $m_c^{\text{pole}}$ | FONLL-B [124] | NLO | 58/52 | 60/52 |
| (NNLO) | 1.275 | $m_c^{\text{pole}}$ | FONLL-C [124] | NLO | 67/52 | 69/52 |
| PDF4LHC15 [8] [d] | – | – | FONLL-B [124] | – | 58/52 | 64/52 |
| | – | – | RT optimal [125] | – | 71/52 | 75/52 |
| | – | – | SACOT($\chi$) [123] | – | 51/47 | 76/47 |

**Accardi, et al. hep-ph/1603.08906**

*No advantage of the GMVFN schemes: the VFN $\chi^2$ values are systematically bigger than the FFN ones*

# *Charm quark mass and the Higgs cross section*

## *MMHT*

- "Tuning" Charm mass $m_c$ parameter effects the Higgs cross section
  - linear rise in $\sigma(H) = 40.5 \dots 42.6$ pb for $m_c = 1.15 \dots 1.55$ GeV with MMHT14 PDFs Martin, Motylinski, Harland-Lang, Thorne '15

| $m_c^{\text{pole}}$ [GeV] | $\alpha_s(M_Z)$ (best fit) | $\chi^2$/NDP (HERA data on $\sigma^{c\bar{c}}$) | $\sigma(H)^{\text{NNLO}}$ [pb] best fit $\alpha_s(M_Z)$ | $\sigma(H)^{\text{NNLO}}$ [pb] $\alpha_s(M_Z) = 0.118$ |
|---|---|---|---|---|
| 1.15 | 0.1164 | 78/52 | 40.48 | (42.05) |
| 1.2 | 0.1166 | 76/52 | 40.74 | (42.11) |
| 1.25 | 0.1167 | **75/52** | **40.89** | (42.17) |
| 1.3 | 0.1169 | 76/52 | 41.16 | (42.25) |
| 1.35 | 0.1171 | 78/52 | 41.41 | (42.30) |
| 1.4 | 0.1172 | **82/52** | 41.56 | **(42.36)** |
| 1.45 | 0.1173 | 88/52 | 41.75 | (42.45) |
| 1.5 | 0.1173 | 96/52 | 41.81 | (42.51) |
| 1.55 | 0.1175 | 105/52 | 42.08 | (42.58) |

# Constraints on strange sea

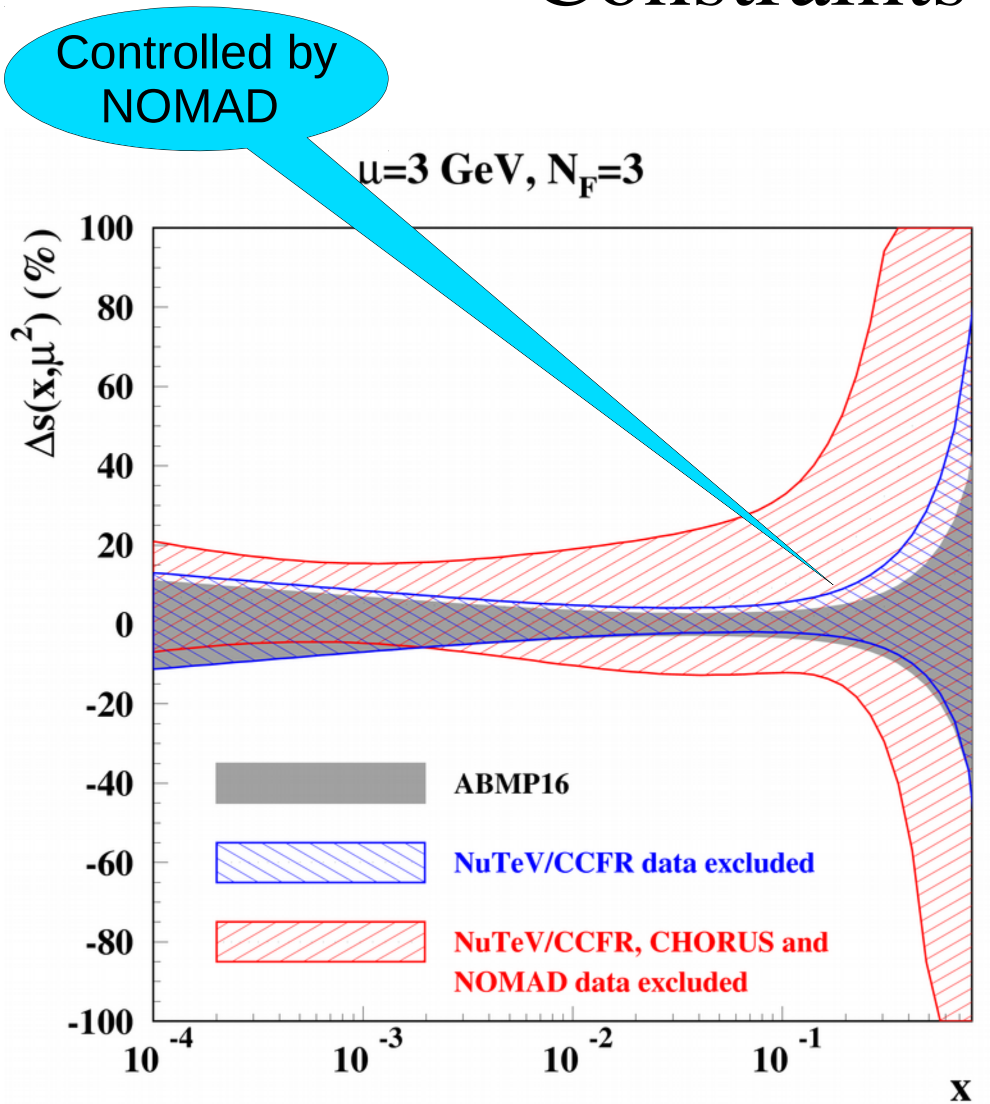


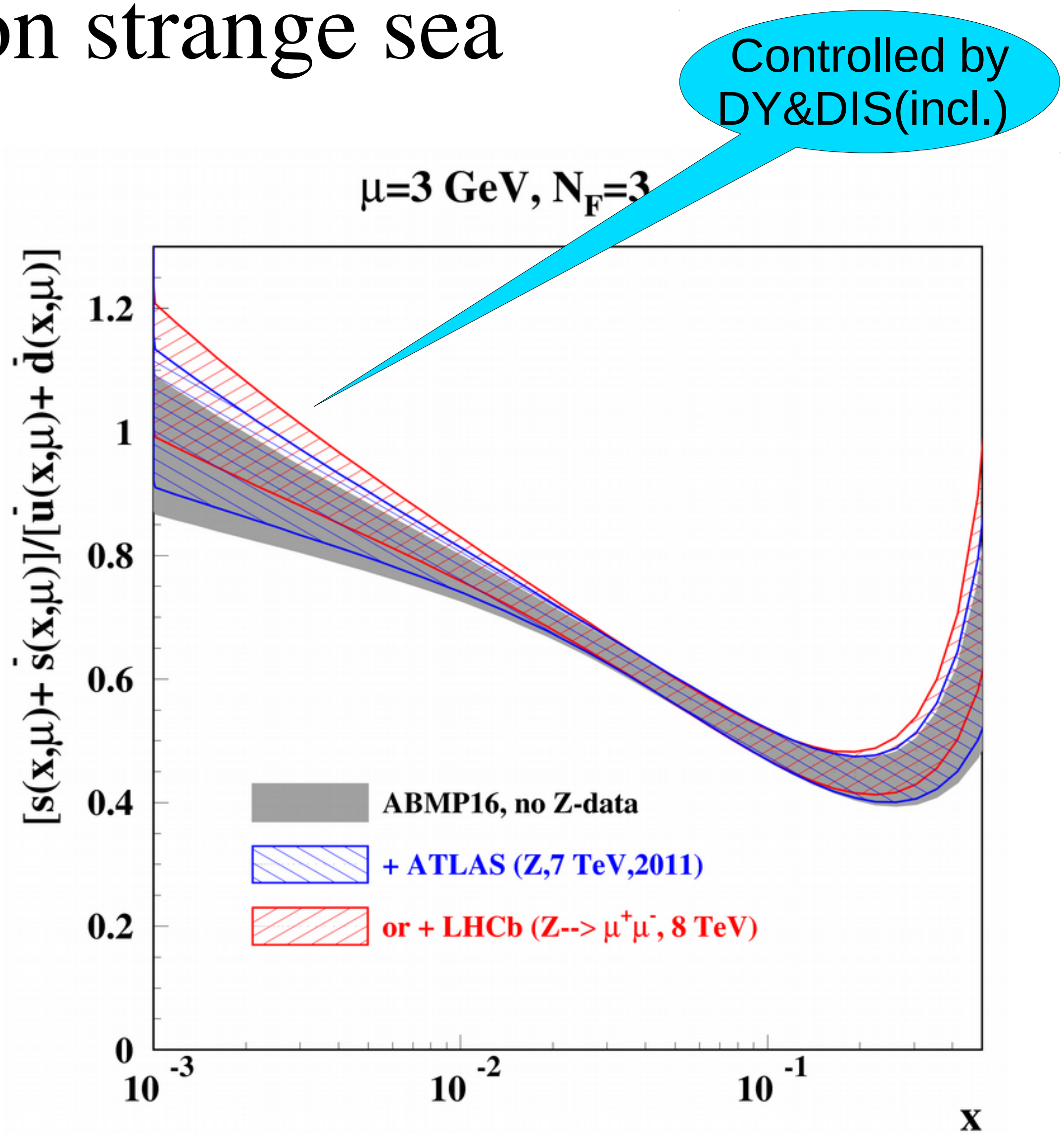


- Uncertainty of ~5% is achieved at x around 0.1
- NuTeV/CCFR data play no essential role → impact of the nuclear corrections is greatly reduced (NOMAD and CHORUS give the ratio CC/incl.)

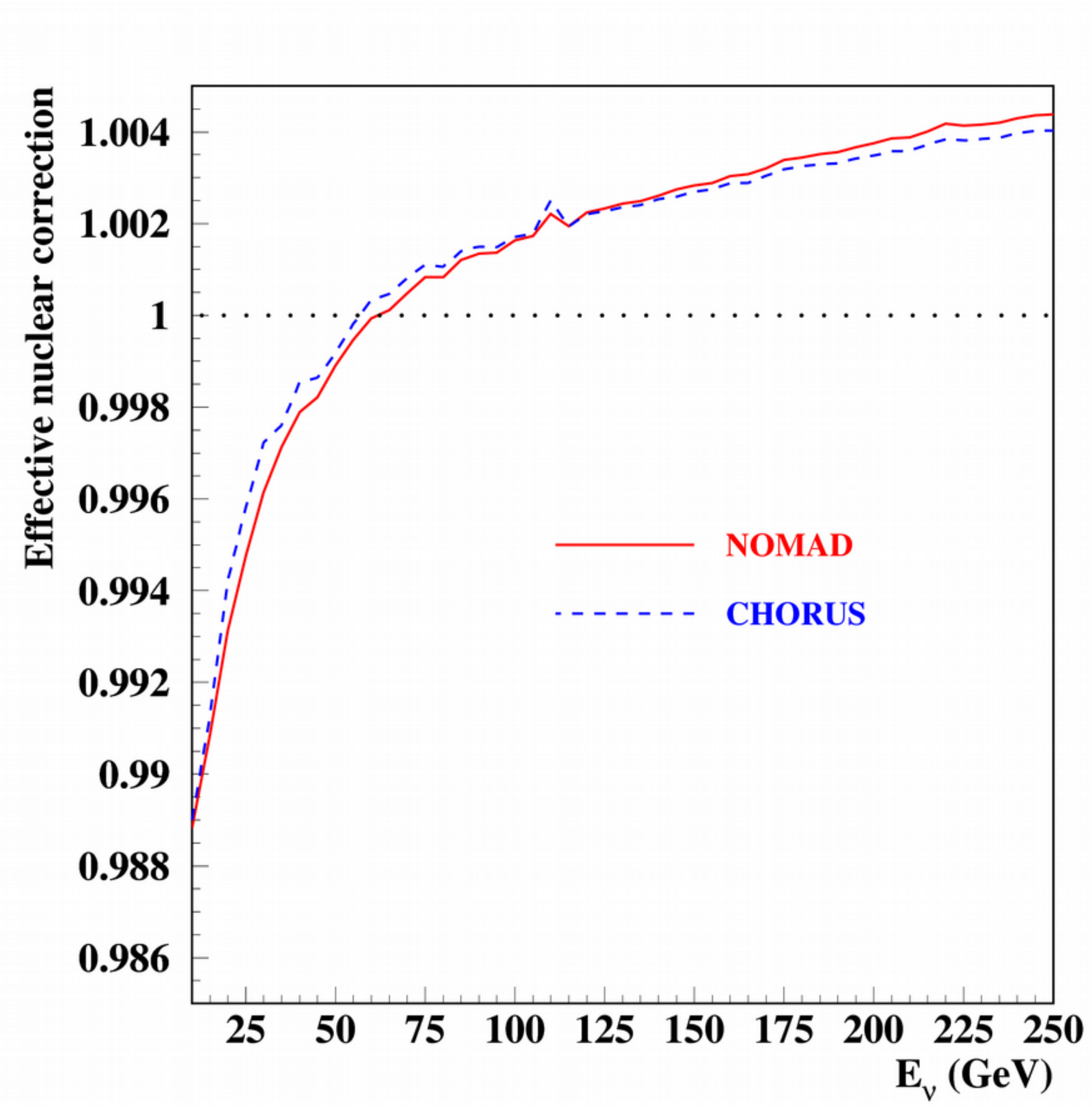

Effective nuclear correction
1.004
1.002
1
0.998
0.996
0.994
0.992
0.99
0.988
0.986
NOMAD
CHORUS
25
50
75
100
125
150
175
200
225
250
$E_\nu$ (GeV)

# CHORUS charm data

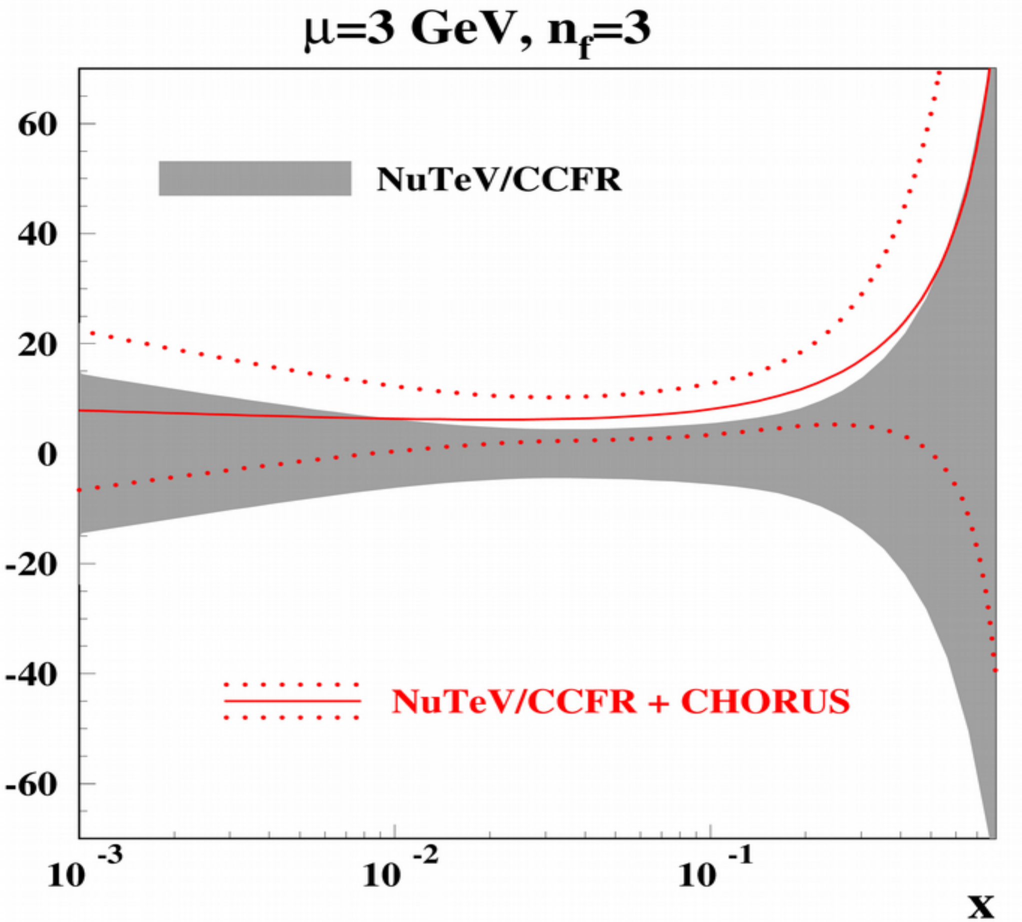


Emulsion data on charm/CC ratio with the charmed hadron vertex measured

**CHORUS NJP 13, 093002 (2011)**

– full phase space measurements

– no sensitivity to $B_\mu$

– low statistics (2013 events)

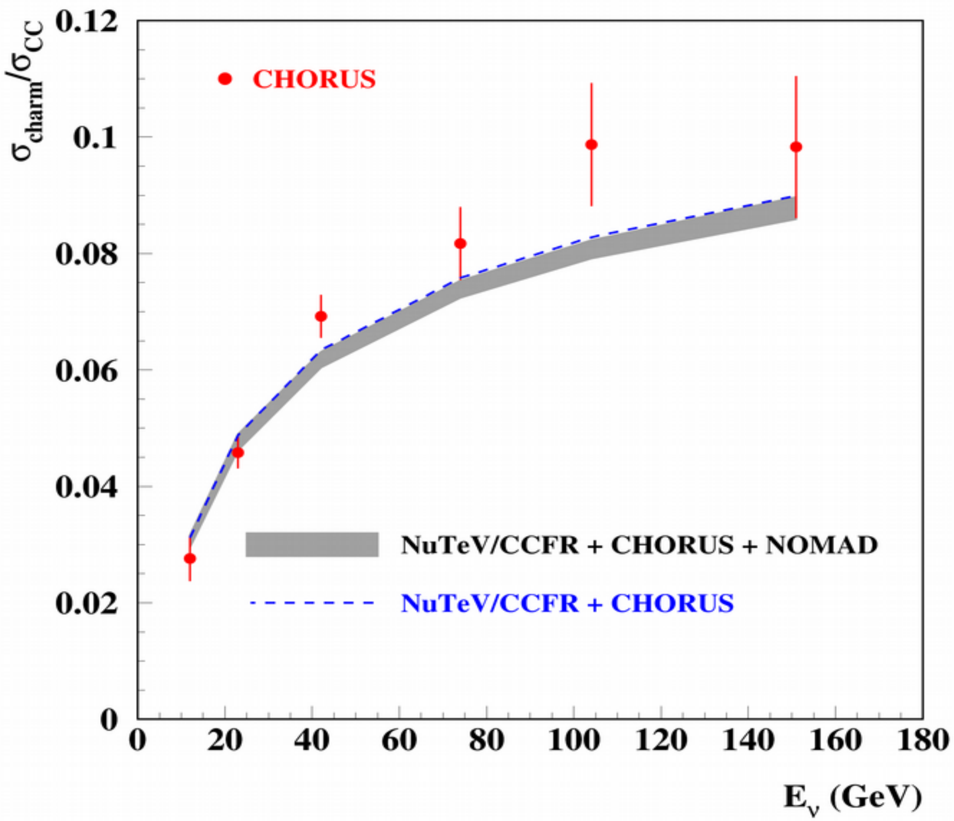


CHORUS data pull strangeness up, however the statistical significance of the effect is poor

**sa, Blümlein, Caminada, Lipka, Lohwasser, Moch, Petti, Placakyte hep-ph/1404.6469**

# CMS W+charm data

CMS Collaboration JHEP 02, 013 (2014)

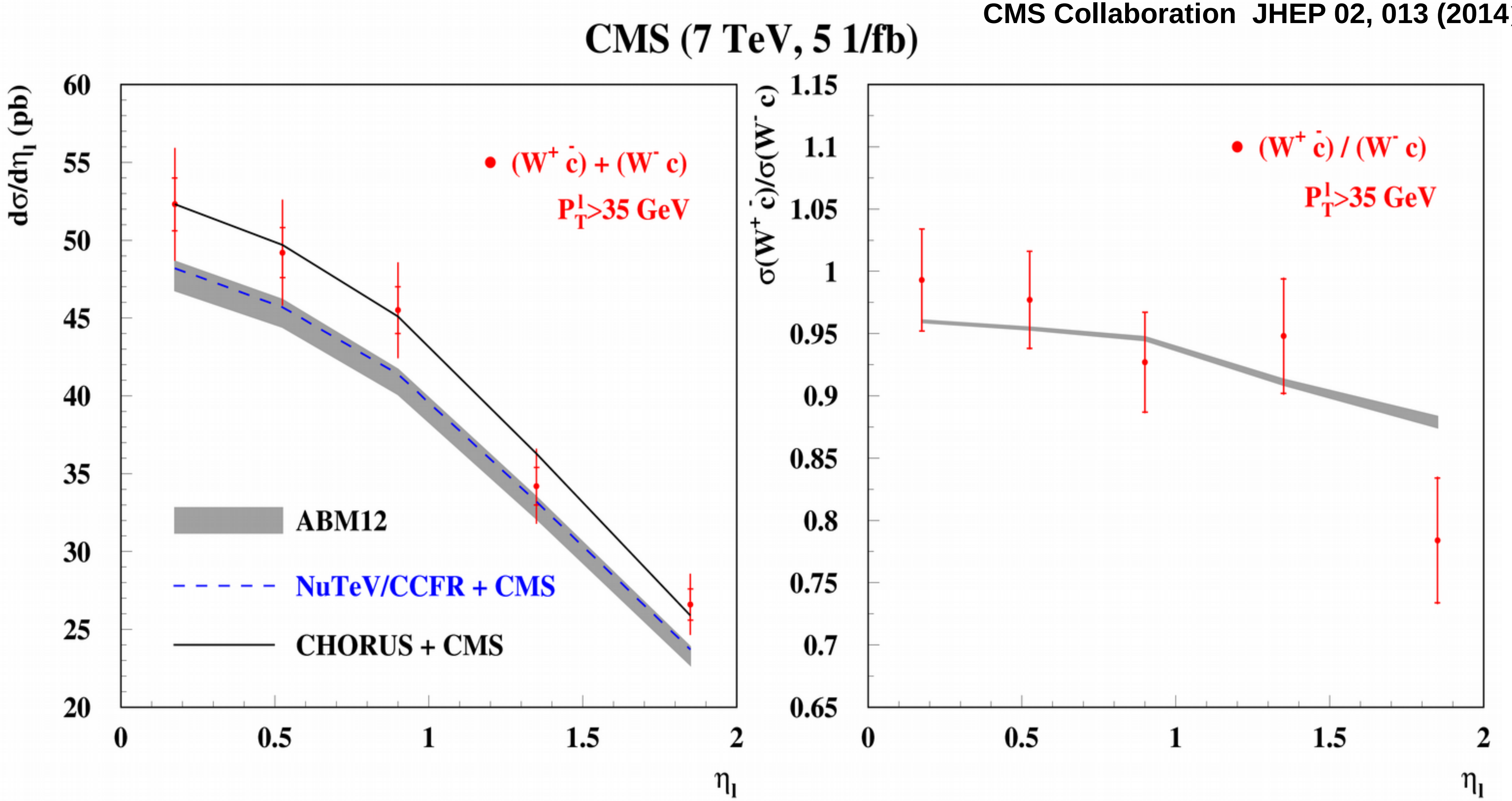


- CMS data go above the NuTeV/CCFR by 1σ; little impact on the strange sea
- The charge asymmetry is in a good agreement with the charge-symmetric strange sea
- Good agreement with the CHORUS data

# ATLAS W+charm data

ATLAS arXiv:1402.6263

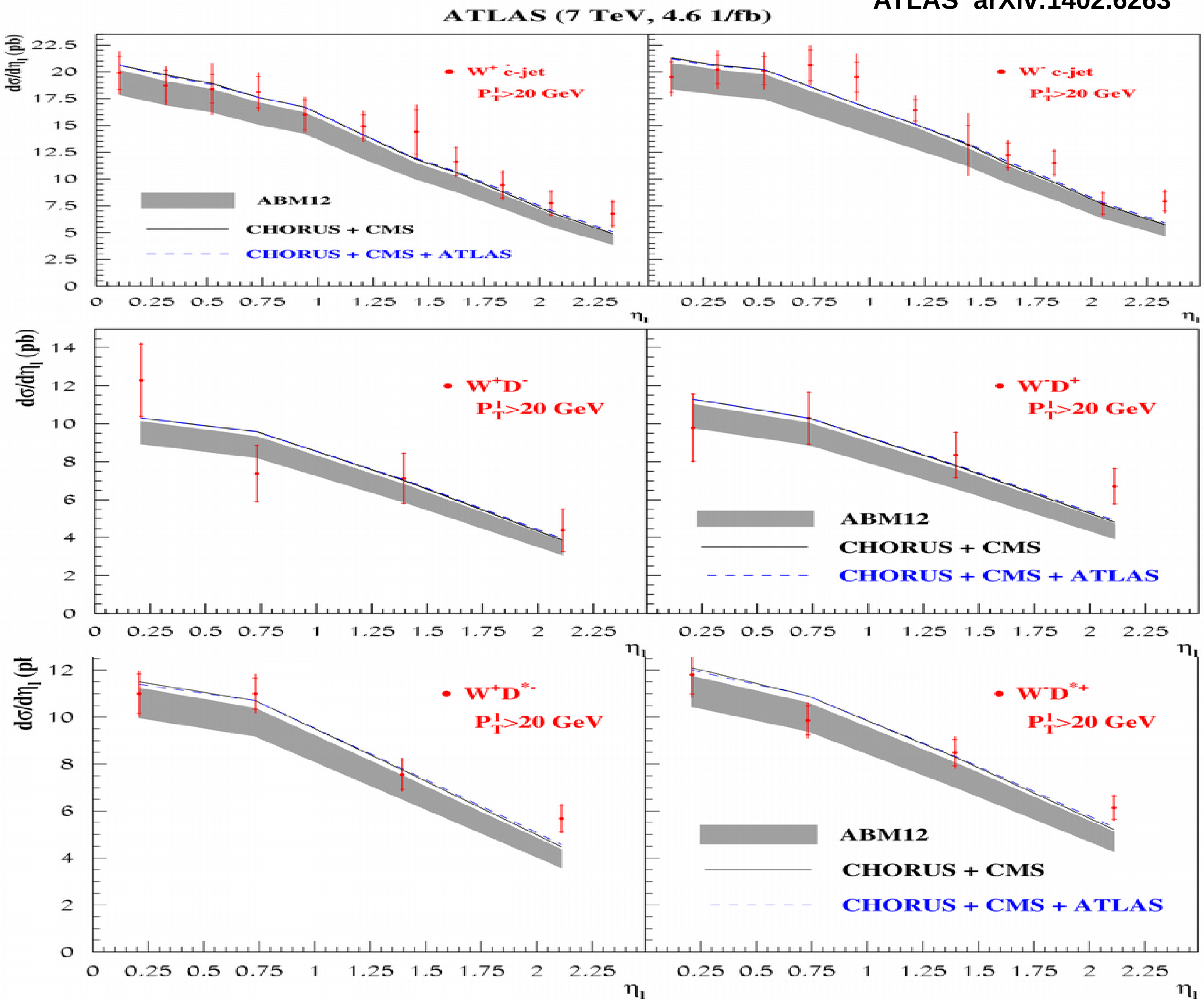

$$(\bar{d}-\bar{u})(x,Q_0^2) = A(1-x)^{\eta_{sea}+2}x^{\delta}(1+\sum_{i=1}^{4} a_i T_i(1-2x^{\frac{1}{2}})),$$



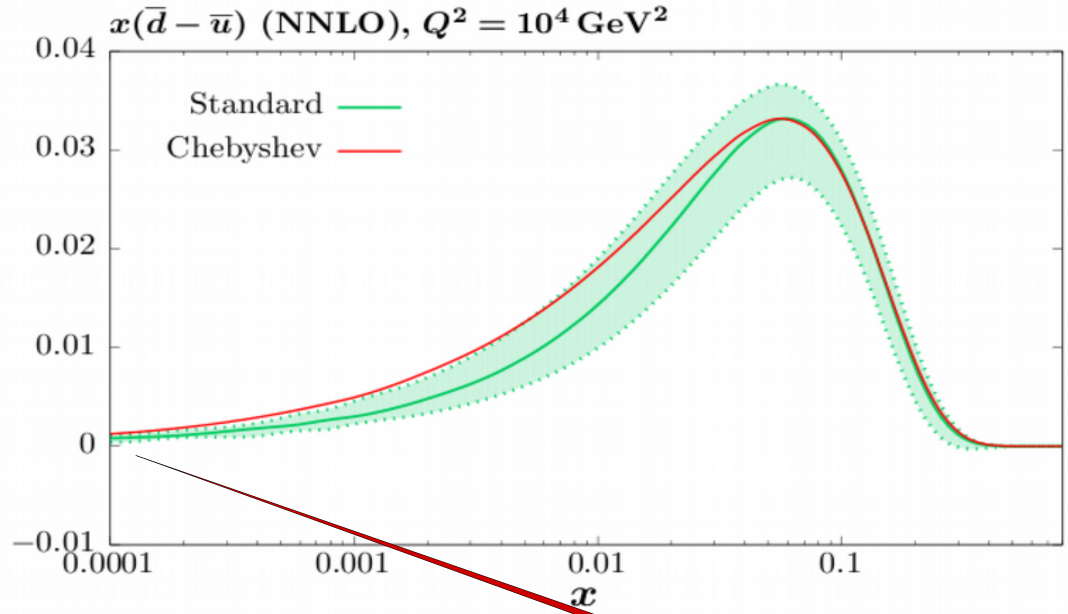


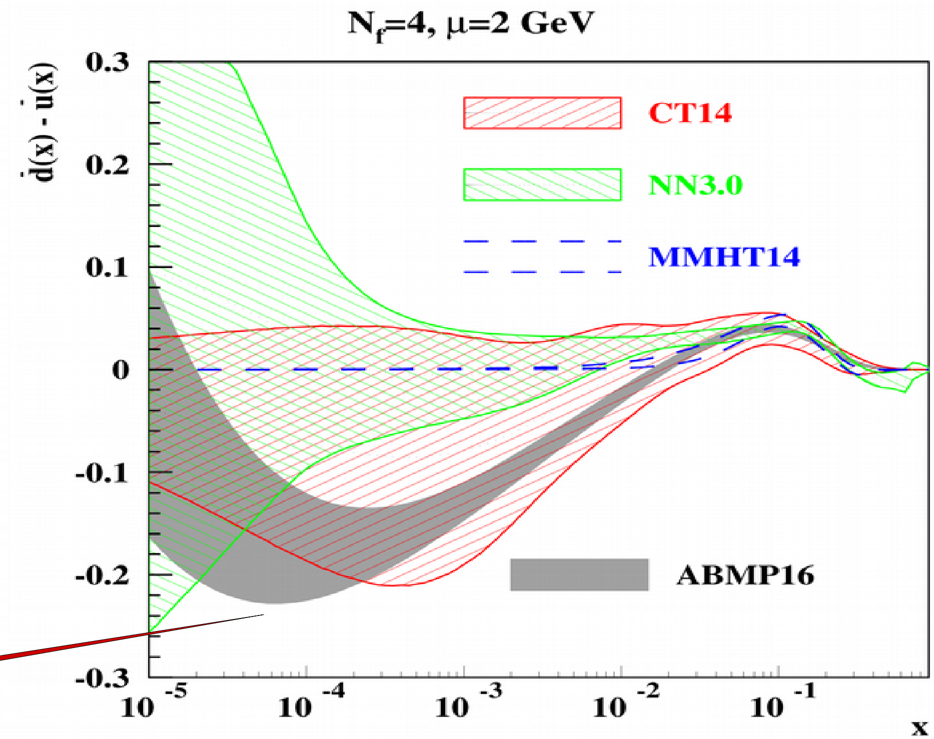


Thorne, this conference

| | no. points | NLO $\chi^2_{pred}$ | NLO $\chi^2_{new}$ | NNLO $\chi^2_{pred}$ | NNLO $\chi^2_{new}$ |
|---|---|---|---|---|---|
| $\sigma_{t\bar{t}}$ Tevatron +CMS+ATLAS | 18 | 19.6 | 20.5 | 14.7 | 15.5 |
| LHCb 7 TeV $W+Z$ | 33 | 50.1 | 45.4 | 37.1 | 36.7 |
| LHCb 8 TeV $W+Z$ | 34 | 77.0 | 58.9 | 76.1 | 67.2 |
| LHCb 8TeV $e$ | 17 | 37.4 | 33.4 | 30.0 | 27.8 |
| CMS 8 TeV $W$ | 22 | 32.6 | 18.6 | 57.6 | 29.4 |
| CMS 7 TeV $W+c$ | 10 | 8.5 | 10.0 | 8.7 | 8.0 |
| D0 $e$ asymmetry | 13 | 22.2 | 21.5 | 27.3 | 22.9 |
| total | 3738/3405 | 4375.9 | 4336.1 | 3768.0 | 3739.3 |

$$xu_s(x,\mu_0^2) = \bar{u}_s(x,\mu_0^2) = A_{us}(1-x)^{b_{us}}x^{a_{us}P_{us}(x)},$$

$$xd_s(x,\mu_0^2) = \bar{d}_s(x,\mu_0^2) = A_{ds}(1-x)^{b_{ds}}x^{a_{ds}P_{ds}(x)},$$

dbar≠ubar at small x
(the same applies for CT14)

The sum of $\chi^2$/NDP for the DY data by LHCB, CMS, and D0 from the table:

184/119 (MMHT16)

171/119 (ABMP16, no filtering), account of other DY data increases the difference

# Sea quark iso-spin asymmetry

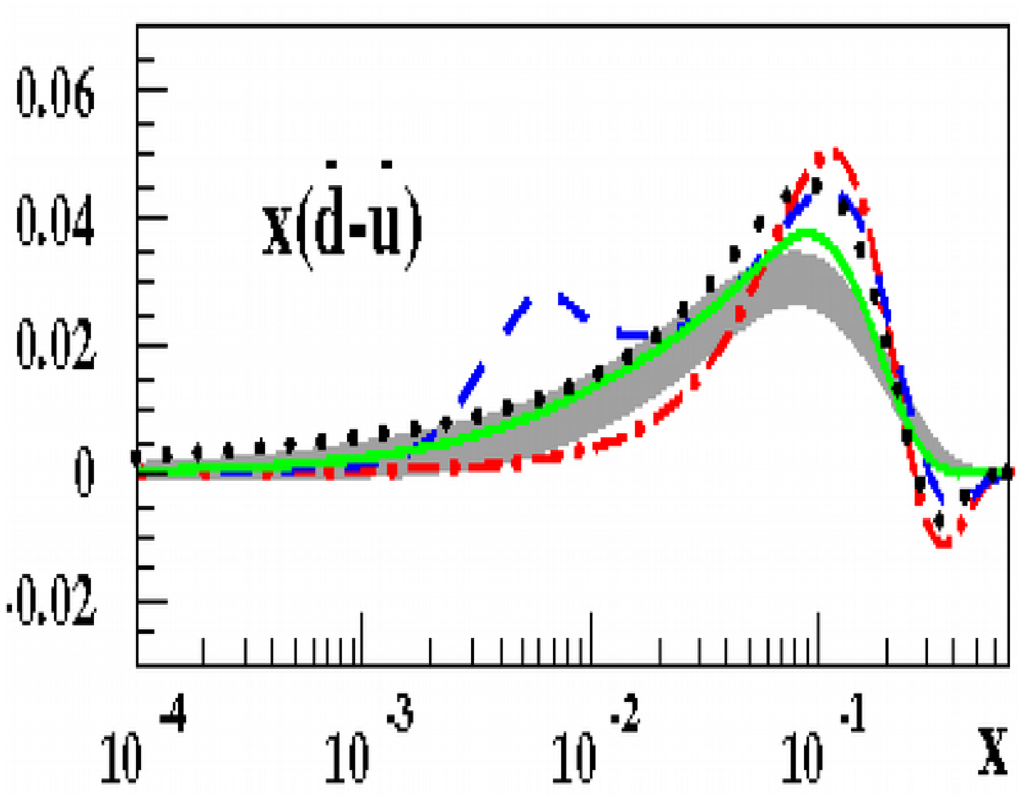


ABM12 CT10 JR09 MSTW08 NNPDF2.3

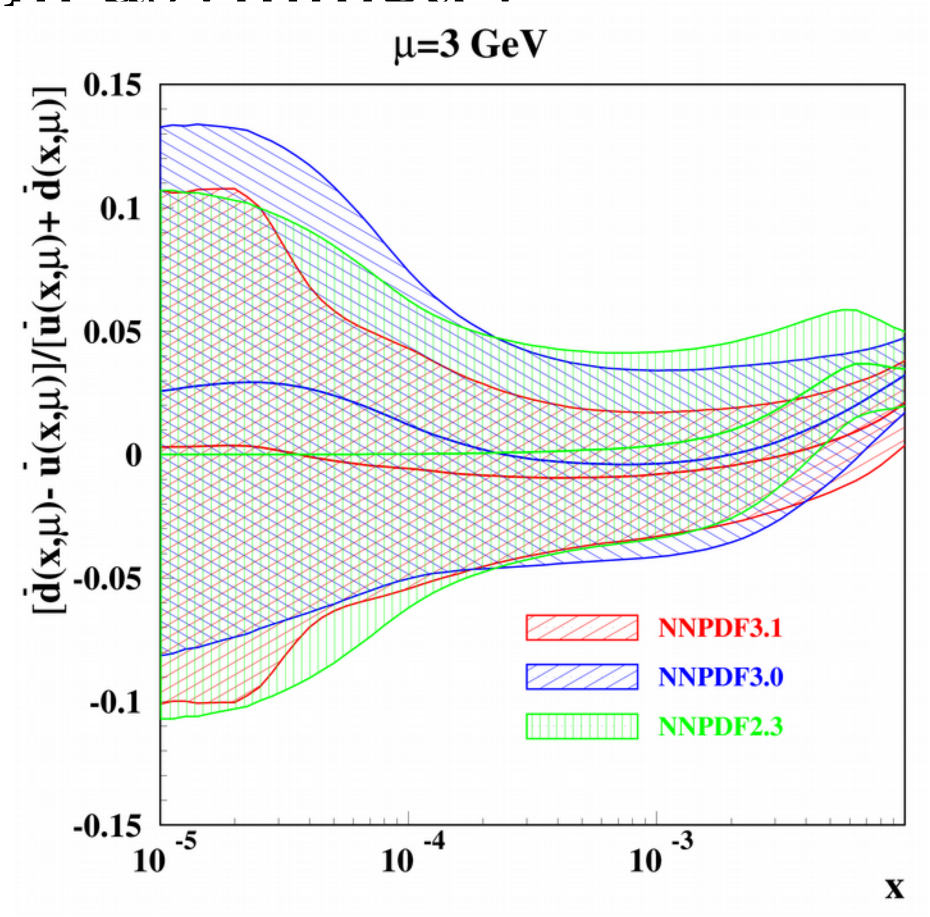


sa, Blümlein, Moch PRD 89, 054028 (2014)

- At x~0.1 the sea quark iso-spin asymmetry is controlled by the fixed-target DY data (E-866), weak constraint from the DIS (NMC)
- At x<0.01 Regge-like constraint like $x^{(a-1)}$, with a close to the meson trajectory intercept; the “unbiased” NNPDF fit follows the same trend

*Onset of the Regge asymptotics is out of control*

# ATLAS W&Z at 13 TeV

ATLAS, hep-ex/1603.09222

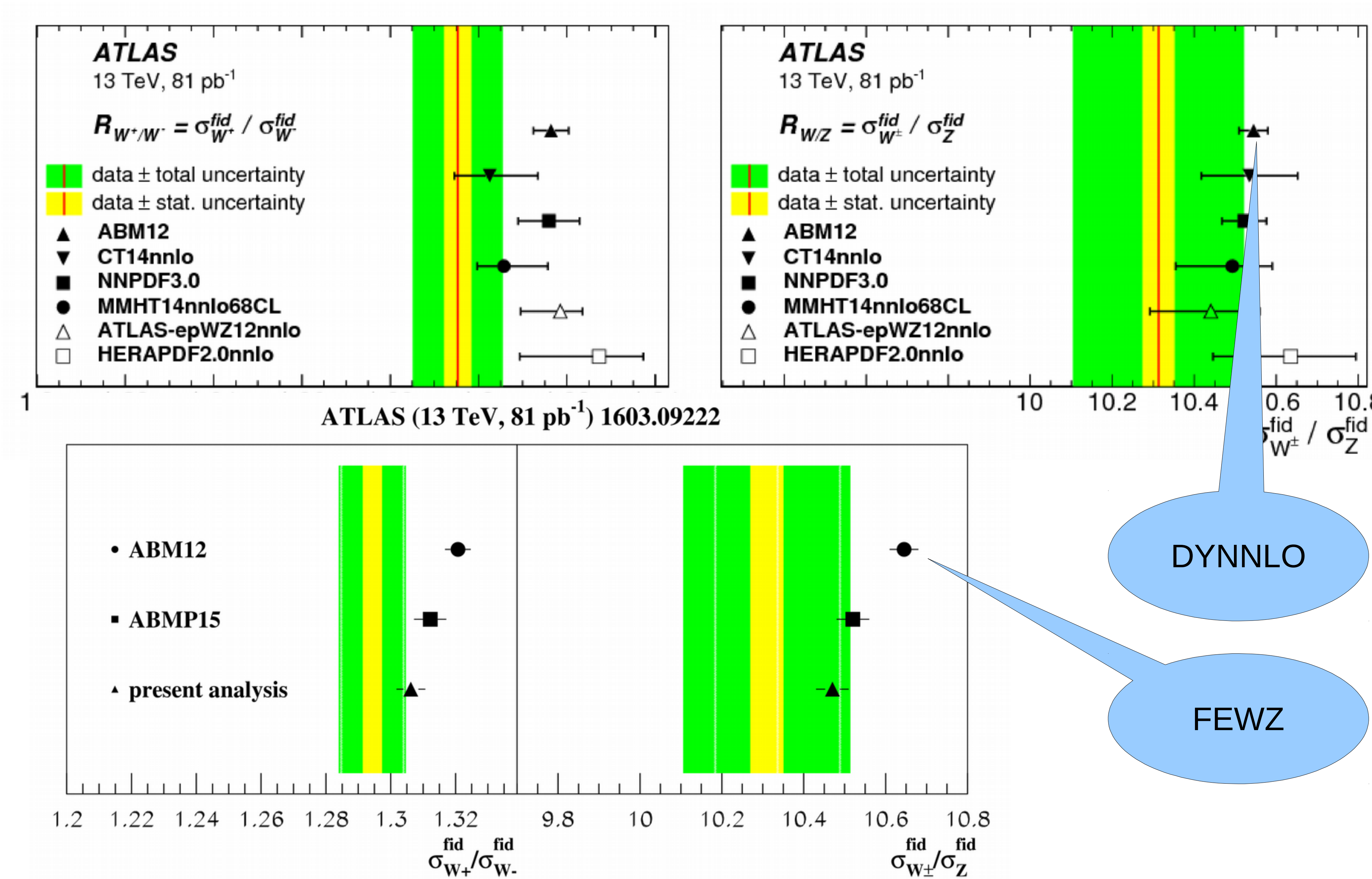


Data are well accommodated into the fit $\chi^2$/NDP=9/6

# Comparison with lattice results

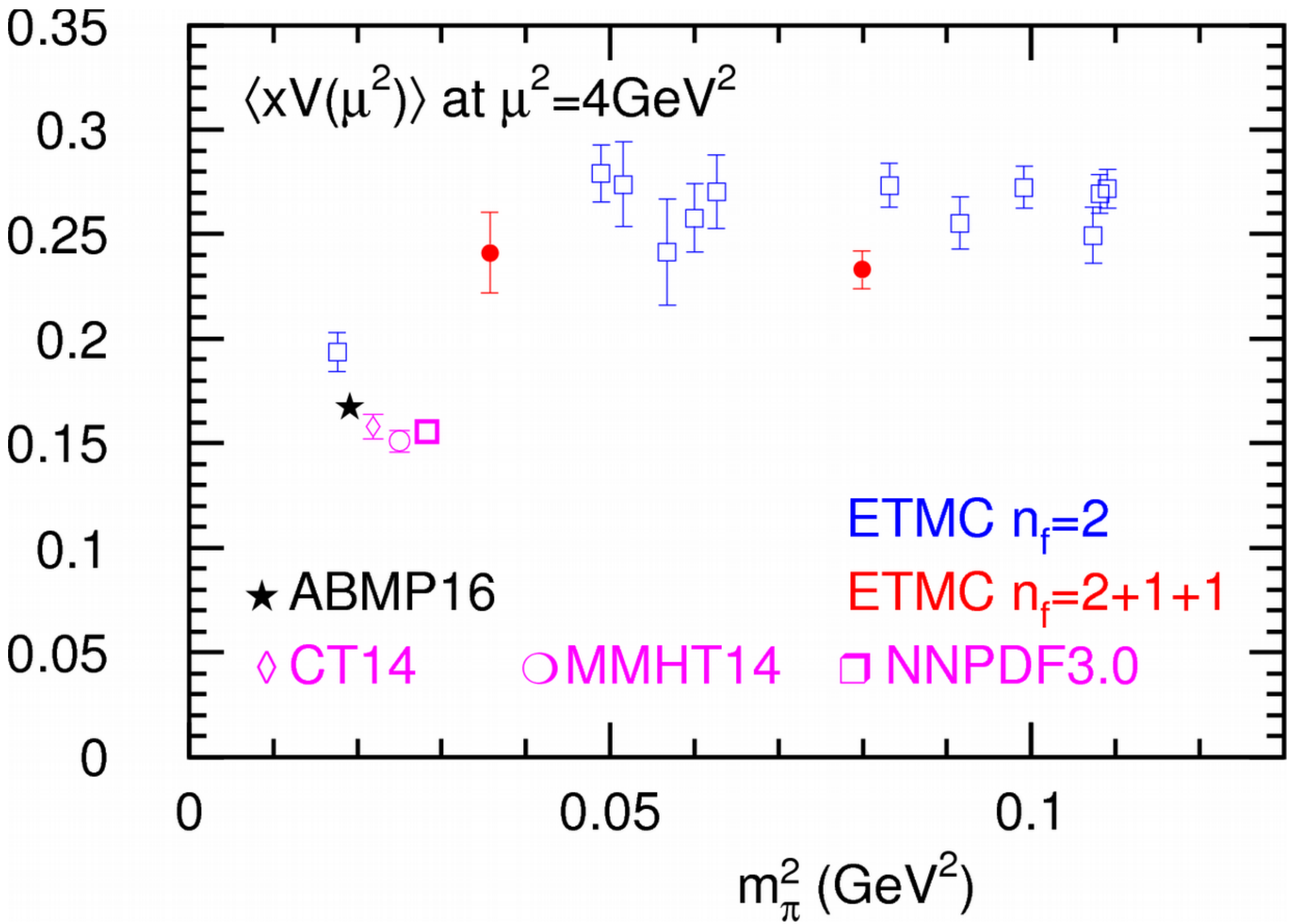

# Details of the epWZ and ABMP16 fits

| | epWZ16 | ABMP16 |
|---|---|---|
| Data | HERA, ATLAS W&Z | HERA, LHC and Tevatron W&Z, fixed-target DIS and charm production, fixed-target DY, …. |
| PDF shape | $xu_v(x,\mu_0^2) = A_{u_v} x^{B_{uv}} (1-x)^{C_{uv}} (1+E_{u_v} x^2)$,<br>$xd_v(x,\mu_0^2) = A_{d_v} x^{B_{d_v}} (1-x)^{C_{d_v}}$,<br>$x\bar{u}(x,\mu_0^2) = A_{\bar{u}} x^{B_{\bar{u}}} (1-x)^{C_{\bar{u}}}$,<br>$x\bar{d}(x,\mu_0^2) = A_{\bar{d}} x^{B_{\bar{d}}} (1-x)^{C_{\bar{d}}}$,<br>$xg(x,\mu_0^2) = A_g x^{B_g} (1-x)^{C_g} - A'_g x^{B'_g} (1-x)^{C'_g}$,<br>$x\bar{s}(x,\mu_0^2) = A_{\bar{s}} x^{B_{\bar{s}}} (1-x)^{C_{\bar{s}}}$,<br><br>15 free parameters | $xq_v(x,\mu_0^2) = \frac{2\delta_{qu}+\delta_{qd}}{N_q^v} (1-x)^{b_{qv}} x^{a_{qv} P_{qv}(x)}$,<br>$xq_s(x,\mu_0^2) = A_{qs} (1-x)^{b_{qs}} x^{a_{qs} P_{qs}(x)}$,<br>$xg(x,\mu_0^2) = A_g (1-x)^{b_g} x^{a_g P_g(x)}$,<br>$P_p(x) = (1+\gamma_{-1,p}\ln x)\left(1+\gamma_{1,p}x+\gamma_{2,p}x^2+\gamma_{3,p}x^3\right)$,<br><br>25 free parameters |

ABMP16 PDFs are selected more flexible in order to accommodate more data as compared to the EpWZ16 fit, which was evolved form the HERA data analysis

# Implication for(of) the single-top production

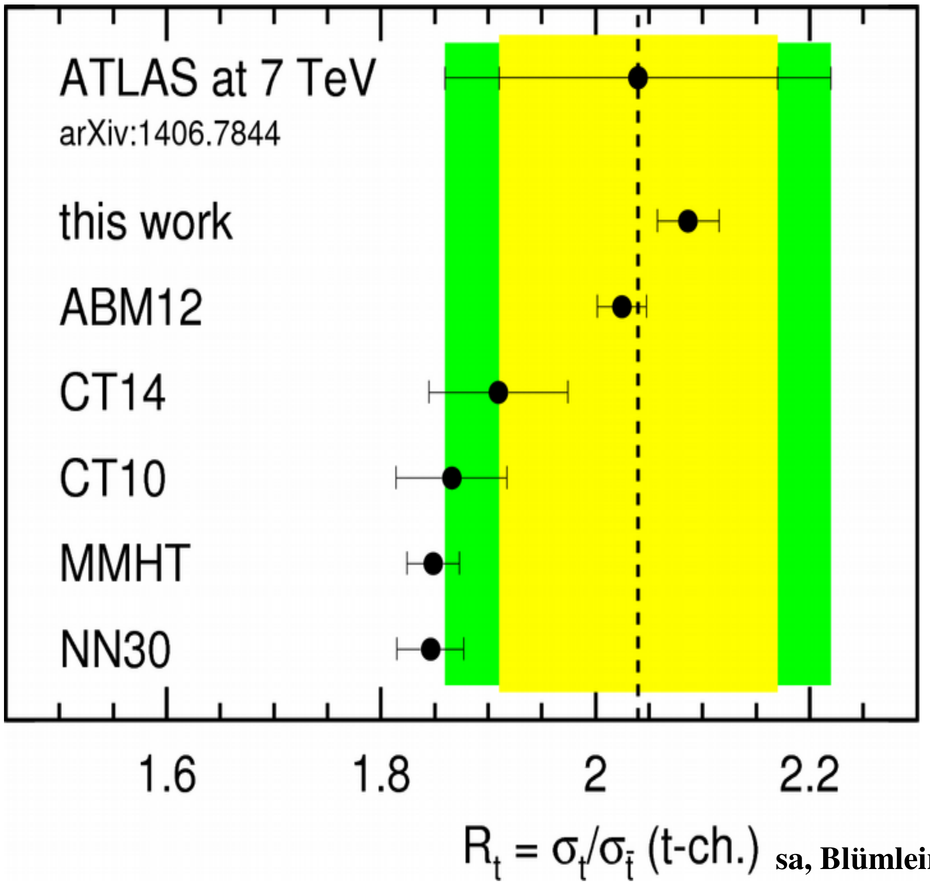


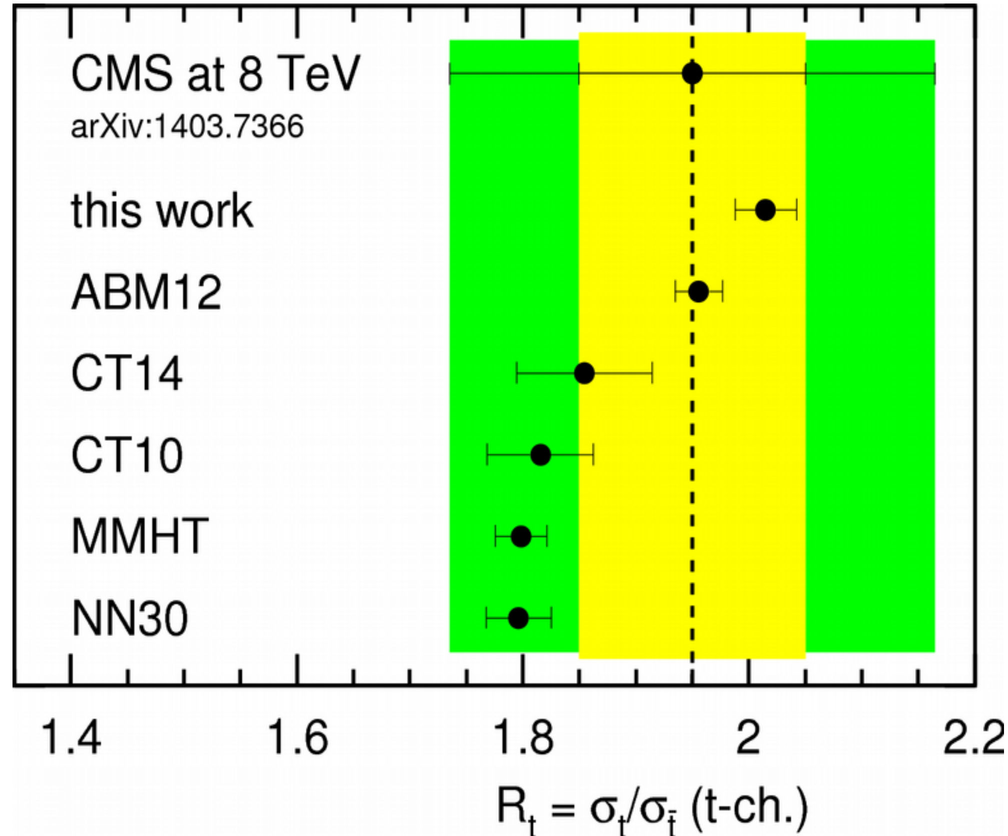


**sa, Blümlein, Moch, Plačakytė hep-ph/1508.07923**

- ATLAS and CMS data on the ratio t/tbar are in a good agreement

- The predictions driven by the froward DY data are in a good agreement with the single-top data (N.B.: ABM12 is based on the deuteron data → consistent deuteron correction was used) **talks by Petti at DIS2016**

*Single-top production discriminate available PDF sets and can serve as a standard candle process*

# Single-top: c.m.s. energy dependence

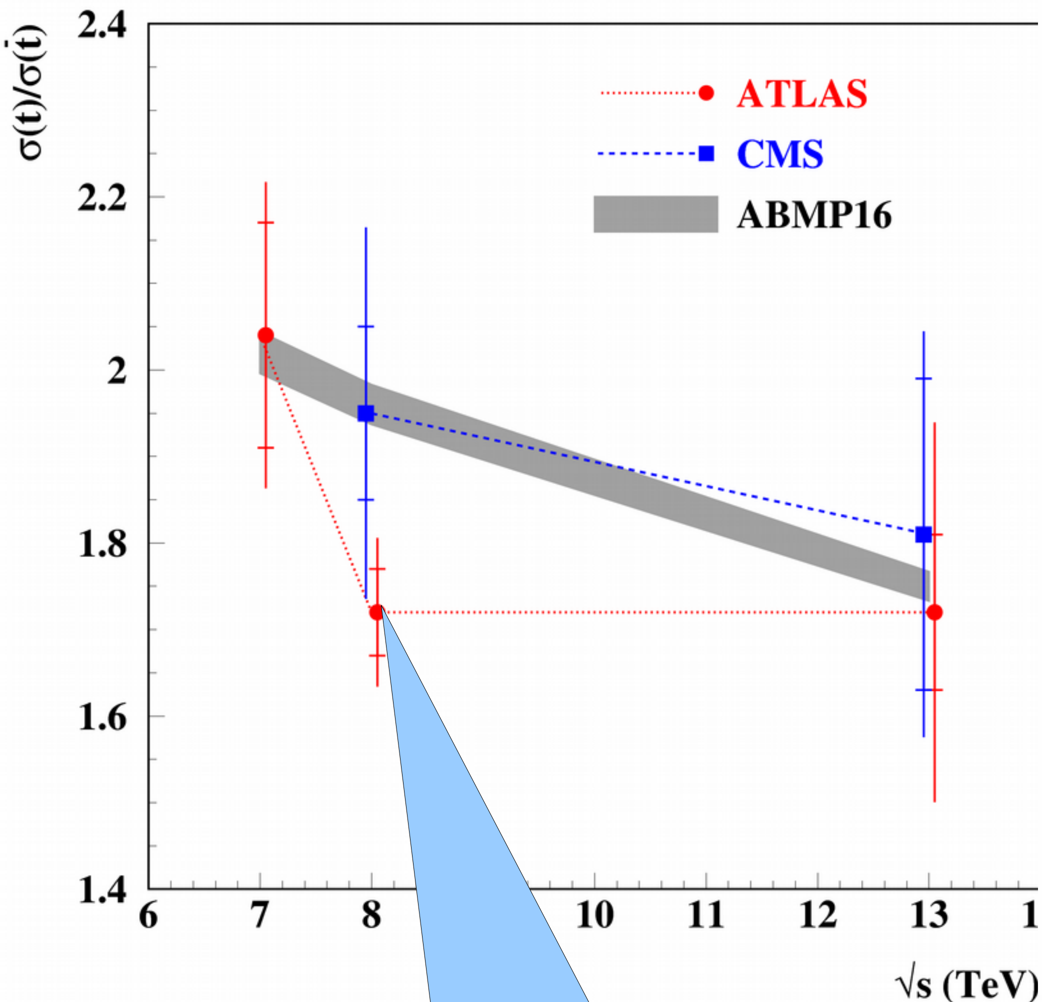


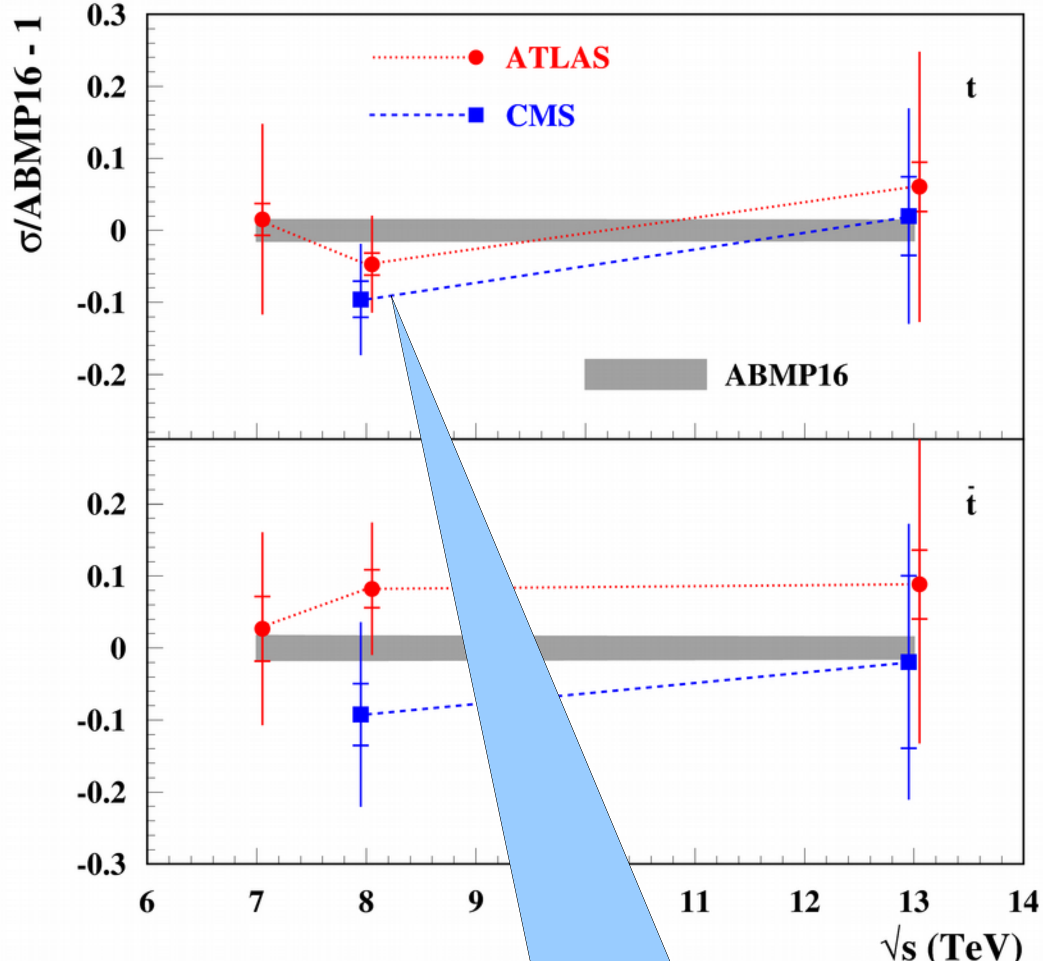


The errors in ATLAS data are much smaller: prefect cancellation of the errors in ratio

The trend in ATLAS data is different for t and tbar samples